A Machine Learning Approach to Evolving an Optimal Propagation Model for Last Mile Connectivity using Low Altitude Platforms

Faris A. Almalki and Marios C. Angelides
Department of Electronic and Computer Engineering
College of Engineering Design and Physical Sciences
Brunel University London
Uxbridge UB8 3PH, United Kingdom
{faris.almalki, marios.angelides}@brunel.ac.uk

***Abstract* - This paper develops a machine leaning framework that evolves an optimal propagation model for the last mile with Low Altitude Platforms from existing propagation models. Existing propagation models reviewed exhibit both advantages and shortcomings in relation to a set of factors that affect performance across different terrains, i.e. path loss, elevation angle, altitude, coverage, power consumption, operational frequency, interference, and antenna type. A comparison of the predictions between the optimized and the existing models in relation to above set of factors reveals significant improvements are achieved with the optimal model.**

Keywords - ***Propagation models; Low Altitude Platforms; Machine learning;***

1 INTRODUCTION

Interest in helium-filled solar-powered airship platforms that operate at altitudes up to 20km above ground is on the increase. High Altitude Platforms (HAPs) have many merits, including a capability of providing regional footprint and a long endurance but their deployment is an expensive option when considering the delivery of wireless communications in remote areas. Therefore, in the case of short-term large-scale events or during and immediately after natural disasters, Low Altitude Platforms (LAPs) are preferred for providing dynamic and scalable networks as they can cover quickly a wide area with a radius running into tens of kilometres, depending on configuration and communication payloads [1-2]. Fig.1 gives an overview of the deployment of a LAP as an aerial Base Station (BS) to serve the last mile. It also shows a propagation model configuration with two path loss components, i.e., Free Space Path Loss (FSPL), and an additive path loss due to shadowing effects.

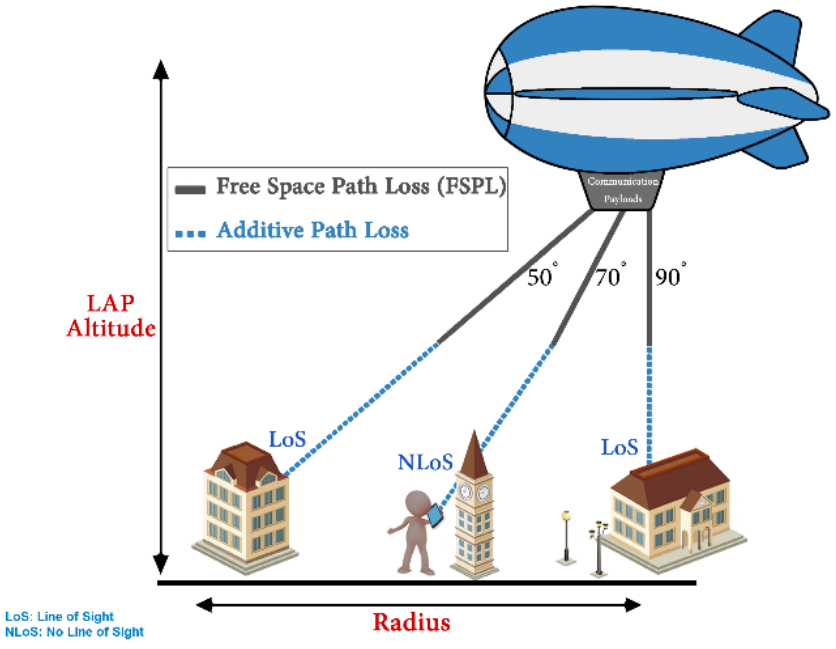

Fig.1: Deploying a LAP as an aerial BS to serve last mile connectivity

Last mile connectivity refers to the maximum distance at which a propagation model may reach users on the ground. This is may be affected by, for instance, the terrain morphology, buildings, trees, interference, fading and atmospheric conditions. Our research review on propagation models reveals several factors that are significant when considering last mile connectivity via LAPs: antenna type, elevation angle, LAP altitude, path loss, coverage area, power consumption, operation frequency and interference. The first three are input factors and the remaining five are output factors. These factors can help with monitoring system performance, network planning, coverage footprint, receivers' line-of-sight, quality of service requirements, and data rates which may all vary across different terrain geomorphologies. Several competing propagation models have been developed over the years but whilst they collectively offer many advantages in relation to the factors, they also exhibit shortcomings across different environments. Therefore, there is no individual or generic propagation model that suits every environment and exhibits optimal performance in relation to all these factors. In our study, four propagation models have been selected that are representatives of their types and exhibit better performance across different terrains in relation to other models.

This paper aims to design a new propagation model for last-mile connectivity with LAPs technology as an alternative to an aerial base station that exhibits optimal performance in relation to the above set of factors above and none of the shortcomings of existing models. The new propagation model is evolved from the four propagation models using a machine learning framework of Neural Networks. The four models are first adapted to include the elevation angle alongside the multiple-input multiple-output antenna diversity gain and deployed at various altitudes. The adaptation enhances their performance.

The rest of this paper is organized as follows: section 2 reviews related work in relation to the set of factors that affect LAP performance, section 3 discusses the selected propagation models, their adaptation and implementation, section 4 discusses the machine learning framework for evolving an optimal propagation model and its implementation, section 5 compares the predictions of the optimised against the adapted models, section 6 follows suit in a wireless sensor network and section 7 concludes.

2 RELATED RESEARCH REVIEW

This section reviews those issues that reportedly affect the performance of a LAP as an alternative to a BS, i.e. path loss, elevation angle, LAP altitude, coverage area, power consumption, operation frequency, interference, and antenna type (gain, height, transmission power, and loss).

2.1 Path Loss

Propagation models predict signal attenuation or path loss as a measure of the power density of an electromagnetic wave as it propagates through space from a transmitter. Calculating path loss is useful for monitoring system performance, network planning and coverage to achieve perfect reception. Many factors may affect a signal when propagating to a maximum distance such as terrain, frequency, transmitter and receiver antenna heights [3]. With aerial platform propagation path loss models, radio signals propagate through free space until reaching the complex ground ubiquitous environment, where shadowing, scattering and other effects occur by nature and/or man-made structures. Thus, it is essential to identify the different type of environments that have been categorized by International Telecommunication Union (ITU) namely: Urban, Suburban, and Rural [2, 4]. Fig.2 shows the conceptual propagation model from a LAP perspective in different environments. In each environment, factors such as path loss, Received Signal Strength (RSS), coverage, and other link budget parameters may vary in response to geometrical and topography characteristics as well as user profiles. [5] introduces a recent comprehensive survey on aerial platforms in relation to propagation models, altitude, coverage, and power consumption. [6] considers how a propagation path loss model for emergency or security applications may lead to network congestion.

The propagation models for LAPs technology reported in literature are broadly based either on empirical propagation [7-10], or Air-To-Ground (ATG) models [2, 4, 11-13]. Empirical propagation models use a pre-defined set of constants and constraints for different topographies, and different geographical factors such as

hills, terrain, streets, and building heights [7, 14, 15]. Models like UI, COST-231, log-distance, ITU indoor & outdoor, WINNER II, Okumura-Hata, and COST Walfish-Ikegami are typical of the types reported widely in the literature. Despite their results accuracy these empirical propagation models exhibit limitations as a result of their limited antenna heights and short transmission distances. ATG with ray tracing exemplify deterministic models with their use of Maxwell's formula and reflection and diffraction laws [14, 15]. The ATG propagation model is reportedly preferred in the literature for LAP deployments, as it yields an improvement in cell capacity and downlink coverage. Path loss in ATG is calculated by using a closed-form method between a LAP and terrestrial receivers based on two key ATG propagation types. The first type is a LoS condition or near-Line-of-Sight condition, the second type is No Line-of-Sight (NLoS) condition, but still receiving coverage with strong reflections and diffractions.

The authors of [16] emphasise that ATG propagation models have not been investigated in detail when compared to other existing terrestrial propagation models. Thus, in their paper they introduce wide range large- and small-scale fading channel models and highlight their limitations. They argue that the main challenge with ATG models is the high altitude at which optimal performance is achieved, as a result of a decreased shadowing effect and the higher transmission power required. Recommendations have been raised in [2, 4] about the significance of investigating various LAP propagation models that yield an optimum altitude and achieve maximum coverage area in different rural or urban environments. Recommendations also are made in [12] about the significance of exploiting environment properties, urban statistics, and bandwidth as they affect considerably LAP capacity and may help with maximizing footprint and throughput whilst maintaining LoS. The authors of [17, 18] present a survey on various propagation models for aerial platforms and highlight their current research trends and as well as underlining their key future insights including the need to consider a machine learning approach to support various aerial platforms operation at low power consumption and wide coverage.

[19] discuses multiple-hop communication and self-organization of multiple UAVs using a free space propagation model. The multi-tiered network can serve heterogeneous networks for both commercial and military applications. The main findings highlight some challenges that face multi-tiered network including coverage gaps scalability and reliability, network formation, network connectivity, information delivery, and energy management. [20] reviews an IoT architecture and service virtualization from different perspectives including aerial platforms. Where the medium is not homogeneous, selecting a propagation of electromagnetic models is significantly important to sustain network connectivity, achieve wide coverage, minimize path loss and power consumption, especially as we are approaching the broader level of 5G technology with high demand of heterogeneous networks. [21] discusses recent advances and future trends with 5G and beyond for aerial platforms with the researchers highlighting the positive correlation between operational aerial platform altitudes and LoS connectivity at different urban environments with path loss and the shadowing effect optimized.

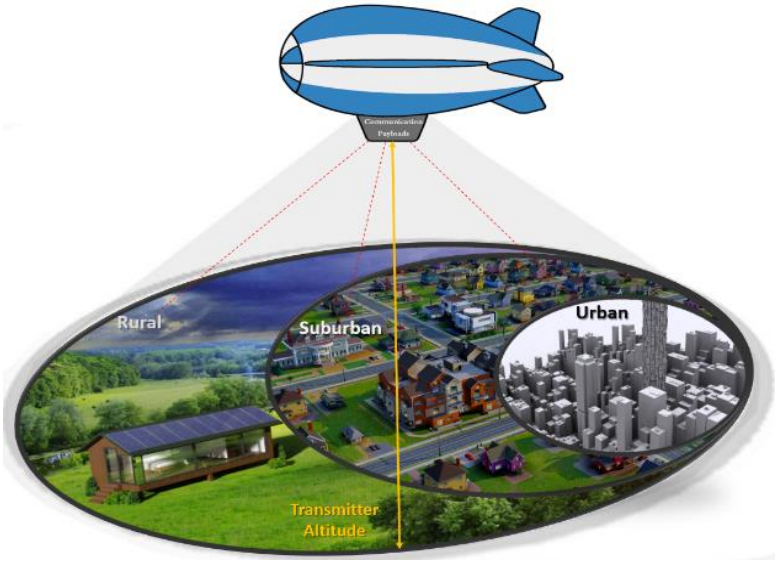

Fig.1: Bird's-eye-view of LAP propagation model in different terrains

2.2 Elevation Angle

It is a necessary condition for ionospheric communication signals to propagate in a correct angle to enhance last mile connectivity. Space-based wireless communication systems take into consideration the elevation angle in their channel FSPL calculation. Nevertheless, there is no consideration of the elevation angle in propagation models reported in literature in relation to LAPs, possibly due to the low transmitter altitude. In aerial platform technology, path loss in a propagation model depends on elevation angle, if aiming to achieve LoS most of the time [2, 4]. Authors of [22, 23] and ITU [24] argue that the elevation angle in urban environments can range between 30° and 90°, 15° and 30° in suburban, and between 5° and 15° in rural. A wide range of elevation angles between 5° and 90° have been investigated in [25] as a function of aerial platforms altitudes in a 3D raytracing propagation model. Their results showcase a clear distinction between LoS and NLoS as elevation angles vary in relation to shadowing fade. In [26] the authors are suggesting that the angle range of 30° to 90° is a realistic elevation range for near space platforms in dense urbans. The proposed model in [11] sets 15° as the minimum elevation angle in urban, as a lower angle range in urban environments would increase the shadowing effect and decrease the probability of a clear LOS path. Moreover, authors in [22] claim that a minimum elevation angle range between 20° to 30° may be more desirable in urban. The authors of [27] consider a 10° elevation angle in addition to altitude, user density and building heights whilst calculating path loss. In [28] authors aim at enhancing the coverage range by choosing a 2° elevation angle at a 320m altitude.

2.3LAP Altitude and Coverage Area

Several wireless network topologies of aerial platforms that provide footprint coverage at different altitudes are reported in the literature. Adopting any topology depends on the Quality of Service (QoS) requirements, type of application, payload weight, and power consumption, each exhibiting its own advantages and challenges [29, 30]. As part of their continuous effort to bridge coverage gaps in wireless communication, researchers in [2, 4, 8, 31, 32] aim at maximising footprint coverage with direct consideration of the LAP altitude in relation to, for instance, maximum allowable path loss (MAPL), RSS, ITU's statistics on urban atmospheric effects such as pressure, wind and temperature, transmission power, and different antenna types. However, issues like power consumption, and the trade-off between coverage and throughput are reported as the main challenges. In [33] the selected propagation models are affected directly by parameters such as carrier frequency and antenna height from both transmitter and receiver sides. The authors in [34] consider various tools of trajectory optimization to analyse the performance of aerial platforms at different aspects, e.g. coverage footprint, throughput, power consumption. They suggest the use of optimization techniques for covering different channel models. [35] proposes a method that tackles the coverage gap that is caused by inefficient planning and deployment of mobile networks. The method is based on a self-deployable mobile network. Results show an average improvement of 50%.

The authors in [16] argue that high altitudes offer larger coverage areas and increased LOS connectivity, but may result in high path loss and higher power consumption. In contrast, low altitude delivers a signal with low path loss, but with increased NLOS and shadowing effects. [36] considers network performance between the Internet of public safety things (IoPST) and drones. The study shows an improvement in the level of public safety in smart cities via measuring LoS probability, delay, and throughput. The results of communication between smart wearable devices and drones show high efficiency and information accuracy. However, the study does not offer details about the altitude of the drones considered or the coverage footprint. [37] offers to reduce the cost of Information-Centric Internet of Things along with enhancing the coverage of communication links between unmanned aerial vehicles (UAVs) and terrestrial receivers via optimization of various parameters such as UAVs altitude, fly duration, power consumption. Their results show an improvement in coverage by approximately 21.42% and reduction in data cost by an average between 13.335% to 34.32%.

2.4 Power Consumption

Unmanned platforms are powered mostly by renewable energy from either directly using photovoltaic or indirectly using concentrated solar power [31, 38]. Power in aerial platforms is mainly consumed by all on-board components and by communication links to terrestrial receivers and other aerial platforms using Radio

Frequency (RF) or optical inter-platform links [4, 7]. Power consumption is an open challenge for other wireless systems including LAP. Therefore, power consumption has received varied considerations with some researchers considering its hardware nature [39, 40] whereas others address the software nature using optimisation techniques [13, 41, 42]. The authors in [16] highlight the relationship between high aerial platform altitude and power consumption that needs to be balanced in consideration of the application and priority. In [34] various optimization techniques are considered to enhance the performance of power consumption at various aerial platforms angles. [21] argues that energy efficiency is a bottleneck challenge for aerial platforms and point at recent developments in battery technologies both in software and hardware. Examples of hardware developments include enhanced lithium-ion batteries, solar energy and hydrogen fuel cells. Examples of software developments include energy beamforming via MIMO techniques. In order to achieve maximum cell coverage for long distances, path loss and aerial platform altitude are considered as opposing aspects.

2.5 Operational Frequency and Interference

The frequency band is one of many factors that affect signal propagation. Authors in [9, 43, 44] argue that the design of propagation models is experimentally driven, hence, the parameters chosen often vary widely but operational frequency seems to be a common choice in consideration of terrain morphology, interference avoidance, and RSS and throughput enhancement. A frequency band of 850 MHz is chosen in [27] based on the availability offered by the cellular operator. Although this yields wider coverage it results in reduced throughput. The ITU's International Mobile Telecommunications-Advanced (IMT-Advanced) standard for 4G offers access to various telecommunication services and supports mobile applications for heterogeneous wireless environments that offer various frequency bands that can support the performance and high QoS requirements for multimedia applications, and high data rates to user and service requirements.

The ITU has long been considering technologies that meet the criteria of the standard: LTE, WiMAX, and WiFi [45-47]. WiFi [10, 44, 48-51], WiMAX [7, 44, 51, 52] and LTE [1, 10, 12, 48, 50, 51] have been considered widely in aerial platform technology in the literature to serve various applications for better coverage, whether in LoS or NLoS, increased capacity and less interference. However, opinions and decisions vary in relation to application types, operational environment and duration and the LAP's onboard communication payloads and power supply. For instance, Aerial Base Stations with Opportunistic Links for Unexpected and Temporary Events (ABSOLUTE) is one of the most important LAP project worldwide that deploys LTE in their specifications [1]. Google balloon projects base their design and telecommunications payloads on LTE technology to provide Internet access globally. However, emergency or security applications considering LTE may lead to network congestion and interference in comparison to WiMAX. Authors in [8, 52-54] emphasize the advantages of WiMAX over LTE-A in supporting military operations in disaster relief environments where users' requirements change rapidly. Yet, WiMAX offers less coverage and data rates in comparison to LTE, and it has large installation and operational costs. WiFi is still a candidate in LAP deployment in increasing connectivity for short distances. The main limitations are vulnerability to interference as it is unlicensed, and it does not serve longer distances, and whilst increasing transmission power may increase coverage, it also raises power consumption and interference. [21] emphasises the use of LTE unlicensed band that has the advantage of direct transmission to terrestrial users.

The authors of [16] argue that the frequency band should be balanced against the altitude to minimize the tropospheric effects such as fading due to temperature, rain or snow. The authors in [55] emphasise the importance of new rules and regulations on aerial platforms frequency identification by the International Telecommunication Union (ITU) Radio Regulation (RR) and International Civil Aviation Organization (ICAO), the two regulatory bodies responsible for frequency assignment and civil flight. On the one hand, low frequency bands of sub 1 GHz may provide extensive coverage which is against RR, but on the other hand, high frequency bands provide high data rates but experience snow/rain attenuation issues like satellites do. In [56], the authors consider both LoS and NLoS from the perspective of antennas and propagation mode. During their experiments they report that in contrast to the 2.4/5 GHz crowded frequency bands, higher frequency bands may be more suitable for commercial aerial platforms.

2.6 Antenna Types

Typical antennas, whether directional or omni-directional are large in size, consume more power, increase interference, and offer small coverage [57, 58]. In contrast, aerial platforms require small-sized antennas, consuming less power, whilst maintaining a high-performance level. The effect of MIMO and smart antennas on near space solar-powered platform performance and capacity is discussed in [29, 40, 59, 60], where it is being argued that the antenna gain need to be optimised, otherwise end-users may experience weak radio across distances running into several miles. The advantages of deploying these antennas include maximizing capacity, improving QoS, extending coverage range, reducing transmission power and relaxing battery requirements, reducing radio signal fading as a result of diversity gain, and maximizing link budget as a result of smooth user tracking with main lobes and interference nulls. Considering the use of either smart or MIMO antenna technology to improve performance is suggested in [61, 62]. The authors of [16] confirm that considering MIMO functionality for aerial platforms, such as Diversity, could enhance the channel capacity and channel performance. MIMO antenna is introduced in [34, 63] to contribute effectively to a heterogeneous and massive number of IoT devices leading to improved wireless connectivity via aerial platforms. In [64], the authors provide a comprehensive survey of channel characterization from aerial platforms perspectives and argue on open challenging issues such as considering NLoS alongside LoS in propagation models to include shadowing effects in channel calculations and MIMO diversity gain to enhance the reliability of communication. [21] argues that energy efficiency can be maintained by using beamforming via MIMO techniques.

Table 1 reports research gaps and current work on last mile connectivity that evolve from the research review. It then uses this to justify our own motivation for pursuing the research underpinning this paper.

Table 1: Related review windup

Areas	***Open Issues***		***Approaches***
	Being Addressed	***Unresolved / Suggestions***	
Propagation Models	• Wider outdoors channel modelling • Two ATG propagation types: LoS and NLoS	• Shadowing effect partially considered • Full link budget considered across various environments	***ATG models***
	• Few outdoor LAP empirical models • Mathematical models empirically drawn across various environments • Wireless network planning	• Limited LAP altitudes • Additional empirical models to be considered	***Empirical models***
Coverage and LAP Altitude	• Optimum LAP altitude calculation using RSS, MAPL and ITU statistics on urban and atmospheric effects • Enhancing RSS and coverage by increasing LAP altitude, transmission power, utilization, or deploying multi-tethered platform topology • Helical directional or omnidirectional antennas for RF channel modelling to improve RSS and LAP coverage	• Trade-off between LAP altitude, RSS and interference in urban environments • Rise in interference as number of LAPs rise in an area • Updating of urban ITU statistics • Interference management between multi-LAPs • Limited LAP altitudes in empirical models • Large size of directional or omnidirectional antennas, power consumption, and increased interference	***RSS***
Antenna Specifications	• Widespread calculation of LAP coverage footprint • Achieving better connectivity at low elevation angles with directive antennas	• Some elevation angles are unsuitable for all environments • Lack of consideration of elevation angle in empirical models due to low transmission altitude	***Elevation Angle***

		• Trade-off between low elevation angles, path loss, coverage • MIMO antennas for high elevation angles may yield better LoS connectivity, reduced path loss and extended coverage	
	• Some consideration of smart/ MIMO antennas impact on improving link budget performance and minimizing interference	• Smart switched beam antennas need to be considered, although difficult to mount on small LAPs • Advanced MIMO antennas may improve performance	***Smart Antenna***
Power Consumption	• Resource allocation that use gaming to minimize power consumption • Dynamic techniques that calculate optimal LAP location, minimize path loss, improve RSS, reduce power consumption	• Trade-off between throughput and power consumption to guarantee fairness amongst users • Optimisation of path loss to minimize transmitting power, and reduce power consumption	***Software***
	• Direction of antenna reduces power consumption • Antennas that serve various frequency bands • Hardware that may reduce power consumption such as batteries, thin solar panels, or propellers	• Antenna direction reduces RSS as altitude rises • MIMO antenna gain diversity may enhance accuracy and reduce power consumption • Some antennas are unsuitable for mounting on small LAPs	***Hardware***
Operation Frequency and Interference	• WiFi, WiMAX, and LTE are widely considered for LAPs in relation to application types, operational environment and duration and LAP onboard communication payloads and power supply	• Vulnerability to interference in unlicensed bands • Limited coverage • Increase in transmission power may increase coverage, but also increase power consumption and interference • Lack of consideration of WiFi HaLow due to immaturity	***WiFi***
		• Large installation and operational costs • Less coverage and data rates than LTE	***WiMAX***
		• Emergency or security applications may lead to network congestion and interference in comparison to WiMAX	***LTE***

3 PROPAGATION MODEL SELECTION AND ADAPTATION

Fig. 3 shows 17 of the propagation models that we have reviewed in detail that are representative of their respective types along with their main parameters of maximum transmission distance, transmitter and receiver antenna heights and high range of frequency band [11, 14, 15, 65-69]. Propagation models that feature an antenna height h_t of less than 0.1km have not been selected, as the LAP altitude ranges between 0.2km and 5km above ground. Some propagation models offer an advantage of high h_t but offer short range of coverage, e.g. ECC-33, low frequency band (Ibrahim-Parsons), limited environment types (e.g. EPM-73), or low perdition accuracy (e.g. ITU-RP.1546).

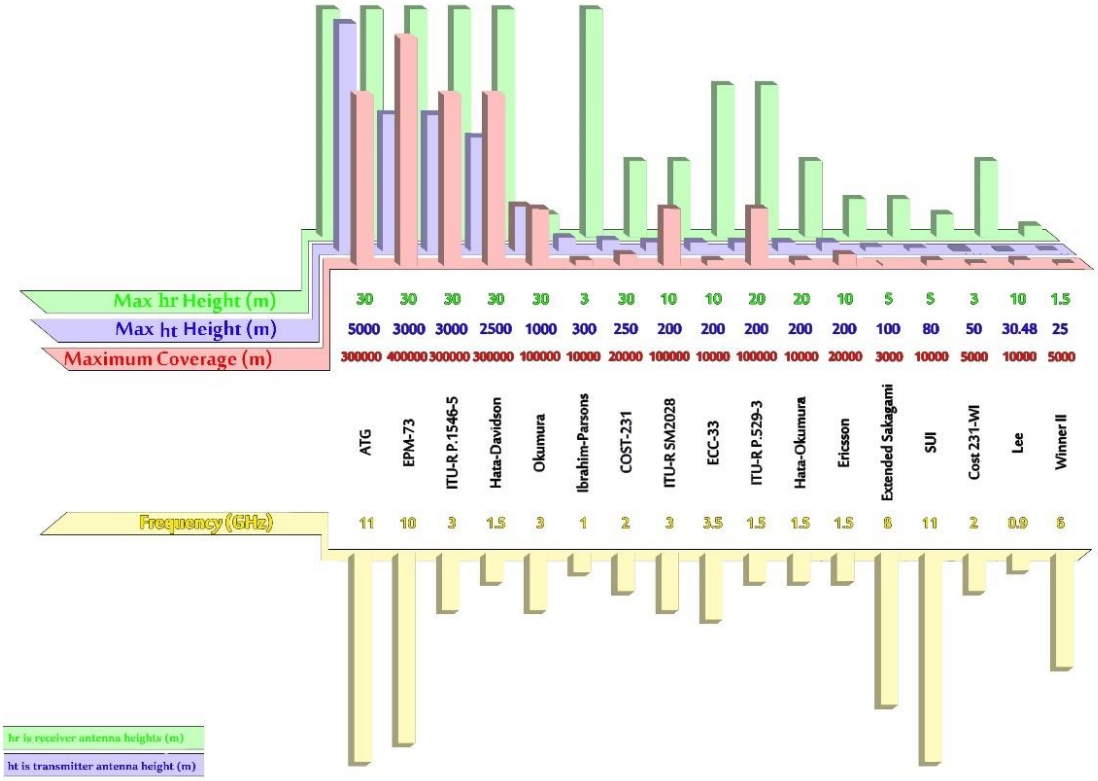

Fig. 3: Landscape of 17 propagation models

Four models that offer advantages of high LAP altitude, antenna high $\boldsymbol{h_t}$, a wide coverage range ≥ 100km, terrain diversity have been selected: ITU-R P.529-3, Okumura, Hata-Davidson, and ATG. All four have the merit of including correction factors that yield high prediction accuracy. Other models also have the same advantages but either yield low perdition accuracy or are not suitable for all terrains [11, 14, 15, 65-69].

3.1 Calculation of Path Loss

Calculation of path loss P_L for ITU-R P.529-3:
Case 1: urban area

$$P_L = 69.55 + 26.16\log(f) - 13.82\log(h_t) - a(h_r) + [44.9 - 6.55\log(h_t)] \times [\log(d)]^b \quad (1)$$

$$a(h_r) = 1.11\log(f) - 0.7(h_r) - [1.56\log(f) - 0.8] \quad (2)$$

$$b = 1 \qquad \text{for } d \leq 20{,}000 \text{ m}$$

$$b = 1 + \left(0.14 + 1.87 \times 10^{-4}(f) + 1.07 \times 10^{-3}(h_t')\right)\left(\log\left(\frac{d}{20{,}000}\right)\right)^{0.8} \quad \text{for } 20{,}000 \text{ m} < d < 100{,}000 \text{ m} \quad (3)$$

$$h_t' = \frac{h_t}{[1+(7\times10^{-6})\times(h_t)^2]^{\frac{1}{2}}} \quad (4)$$

Case 2: suburban area

$$P_L = P_{L(\text{urban})} - 2[\log\left(\frac{f}{28}\right)]^2 - 5.4 \quad (5)$$

Case 3: rural areas

$$P_L = P_{L(\text{urban})} - 4.78[\log(f)]^2 + 18.33\log(f) - 40.49 \quad (6)$$

Calculation of path loss P_L for Okumura:

$$P_L = L_f + Amn(f,d) - G(h_t) - G(h_r) - G_{\text{area}} \quad (7)$$

$$L_f = 32.44 + 20\log(f) + 20\log(d) \quad (8)$$

$G(h_t)$= 20 log (h_t/200), 10m< h_t<1000m (9)
$G(h_r)$ =10 log (h_r/3), $h_r \leq$ 3m (10)
$G(h_r)$ =20 log (h_r/3), 10 >h_r>3m (11)

Calculation of path loss P_L for Hata-Davidson:

$$P_L = P_L\text{Hata} + A\,(h_t, d) - S_1(d) - S_2(h_t, d) - S_3(f) - S_4(f, d) \quad (12)$$

where:

$$P_L\text{Hata} = 69.55 + 26.16\log(f) - 13.82\log(h_t) - a(h_r) + [44.9 - 6.55\log(h_t)]\log(d) \quad (13)$$

Case 1: for urban area

$$a(h_r) = (3.2[\log(11.75 \times h_r)]^2) - 4.9 \quad (14)$$

Case 2: for sub-urban, or rural areas

$$a(h_r) = (1.1\log(f) - 0.7)(h_r) - (1.56\log(f) - 0.8) \quad (15)$$

Calculation of path loss for ATG:

$$PL_T = \rho_{LoS} \times PL_{LoS} + \rho_{NLoS} \times PL_{NLoS} \quad (16)$$

The probability of having LoS connections at an elevation angle θ is given by:

$$\rho_{LoS} = a - \frac{a-b}{1+[\frac{\theta-c}{d}]^e} \quad (17)$$

$$\rho_{NLoS} = 1 - P_{LoS} \quad (18)$$

The path loss for LoS and NLoS are:

$$PL_{LoS}\,(dB) = 20\log\frac{4\pi(f)(d)}{c} + \eta_{LoS} \quad (19)$$

$$PL_{NLoS}\,(dB) = 20\log\frac{4\pi(f)(d)}{c} + \eta_{NLoS} \quad (20)$$

where P_L: Path Loss (dB), f: Carrier Frequency (GHz), h_t: Transmitter Antenna Height (m), h_r: Receiver Antenna Height (m), d: Distance (m), $a(h_r)$: Antenna Correction Factor, h_t' correction factor for LAP height h_t, *Lf*: Free Space Path Loss (dB), Amn (*f, d*): Median Attenuation Relative to Free Space (dB), $G(h_t)$: Transmitter Antenna Height Gain Factor (dB), $G(h_r)$: Receiver Antenna Height Gain Factor (dB), G_{area}: Gain due to Type of Environment (dB), P_LHata: Path Loss of Hata Model (dB), $a(h_r)$: Correction Factor for mobile antenna height, A, S_1: factors that extend distance to 300,000m, S_2: correction factor for height h_t of base station antenna extending the value of h_t to 2500m, S_3, S_4 : correction factors that extend frequency to 1.5 GHz, a, b, c, d and e are ITU-R parameters for the three types of environments, θ: Elevation Angle in degrees depends on environment type, η_{LoS}, η_{NLoS}: average additional loss to free space depending on environment type. η_{LoS} ranges between 3 to 5dB, whereas η_{NLoS} ranges between 8 to 12dB.

3.2 Calculation of Link Budget Parameters

Prediction of RSS, coverage, SNIR, and optimum altitude are reported in [48, 71, 72]. RSS depends on transmitter power (P_t), path loss (P_L), transmitter antenna gains (G_t), receiver antenna gains (G_r) as well as (L) connector and cable loss. RSS for cellular network is expressed in dBm as:

$$RSS = P_t + G_t + G_r - P_L - L \quad (21)$$

The footprint from a LAP altitude can be derived from the path loss and RSS results. SNIR is RSS (dB) over N: Noise figure (dB) plus I: Interference (dB):

$$SNIR\,(dB) = \frac{RSS}{N+I} \quad (22)$$

There is no formula with which to calculate the exact throughput based on P_L and SINR. However, a prediction can be made using Shannon's formula. Thus, predicted throughput (C) in bits per second (b/s) is predicted as:

$$C = B \times \log(1 + SNIR) \quad (23)$$

where BW: bandwidth (MHz), SINR: linear power ratio not dB.

When providing coverage of a large area, it becomes increasingly necessary to consider the earth's curvature and radius. An adaptation that has been considered in our work takes into account the elevation angle to the

LAP's quasi-stationary condition, at various LAP altitudes. This adaptation yields improved LoS service connectivity, coverage range, and RSS and QoS service to receivers that would normally experience outage or low connectivity as a result of their distance, the earth's curvature, or terrain morphology. Fig. 4 shows the trigonometric geometry for a LAP, whereby distance D of the selected propagation models is computed.

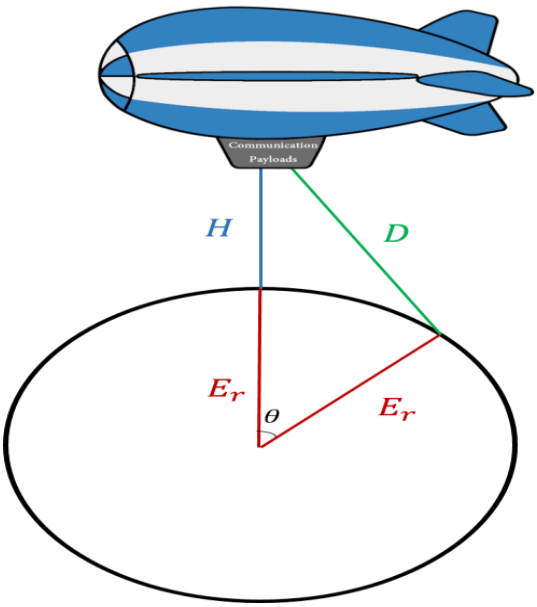

Fig. 4: Trigonometric geometry for a LAP

Given a LAP's altitude H, E_r is the Earth's radius at 6378 km, and θ is the elevation angle from a user's location using ITU's environmental factors for urban, suburban, or rural terrains:

$$\cos\theta = \frac{E_r}{E_r+H} \tag{24}$$

$$\theta = \cos^{-1}\frac{E_r}{E_r+H} \tag{25}$$

$$D = \theta . E_r \tag{26}$$

$$D = 2\,E_r[\cos^{-1}\left(\frac{E_r}{E_r+H} * \cos(\theta)\right) - \theta] \tag{27}$$

The literature offers various considerations and assumptions with regards to selecting an appropriate elevation angle that suits an environment. The assumptions drawn from literature is to set the elevation angles of 15°, 10°, 5° as thresholds in urban, suburban, and rural environments respectively, where the LAP is in a quasi-stationary position.

3.3 Adapted model implementation

Each of the four selected models estimates values for path loss, RSS, SINR, throughput, and coverage or footprint which correlate respectively to the five output performance factors, i.e. path loss, power consumption, interference, capacity and coverage. Path loss is the reception performance indicator. RSS is the power strength indicator and is used to estimate the coverage range when the signal weakens as the receiver moves away from the transmitter. RSS depends on path loss, transmitter and receiver height and gain and environment factors. The SINR is the interference performance indicator and is used to measure the quality of a wireless link and bit error ratio. Throughput is the capacity performance indicator, and decreases with path loss, distance, and shadowing [7, 71, 72]. The four propagation models are simulated under the same conditions using MATLAB. Whilst the transmitter antenna height h_t will vary, the receiver antenna height h_r is set at 5m, as this has been widely adapted in the reviewed literature as well as in the data provided by Airspan WiMAX. Table 2 shows the simulation parameters that relate to MIMO antenna specifications as used by Airspan's 3.5GHz WiMAX [69, 73].

Equations (1) through to (27) are simulated in MATLAB under the same conditions using the link budget specification of Table 2. The simulation has considered two types of receivers based on antenna gains for Base station (BS), and Handset (HS). Simulated predictions are shown first as line graphs on Fig. 5 through to Fig. 16. The altitude chosen (0.2, 1, 2.5, 5) km above the ground are representative altitudes across the full range for transmitter antenna altitude h_t. Coverage footprint in all four models is based on an elevation angle from a user's location which is a significant departure from current empirical models.

Table 2: WiMAX MIMO antennas

Parameters	Value
Frequency band [GHz]	**3.5**
Bandwidth [MHz]	**10**
Modulation type	**QPSK**
Noise figure [dBm]	**6**
Transmitter side	
Transmitter Power [dBm]	**40**
Transmitter Antenna Gain [dBi]	**17**
Diversity gain [dBi]	**6**
Transmitter Rx Sensitivity [dBm]	**-88.9**
Interference margin loss [dB]	**3**
Connector loss [dB]	**0.3**
Receiver side	
Receiver Power [dBm]	**27**
Receiver Antenna Gain [dBi] (stations)	**15**
Receiver Antenna Gain [dBi] (handset)	**2**
Diversity gain [dBi]	**3**
Receiver Rx Sensitivity [dBm]	**-90.9**
Interference margin loss [dB]	**3**
Connector loss [dB]	**0.1**
Body loss [dB]	**0**

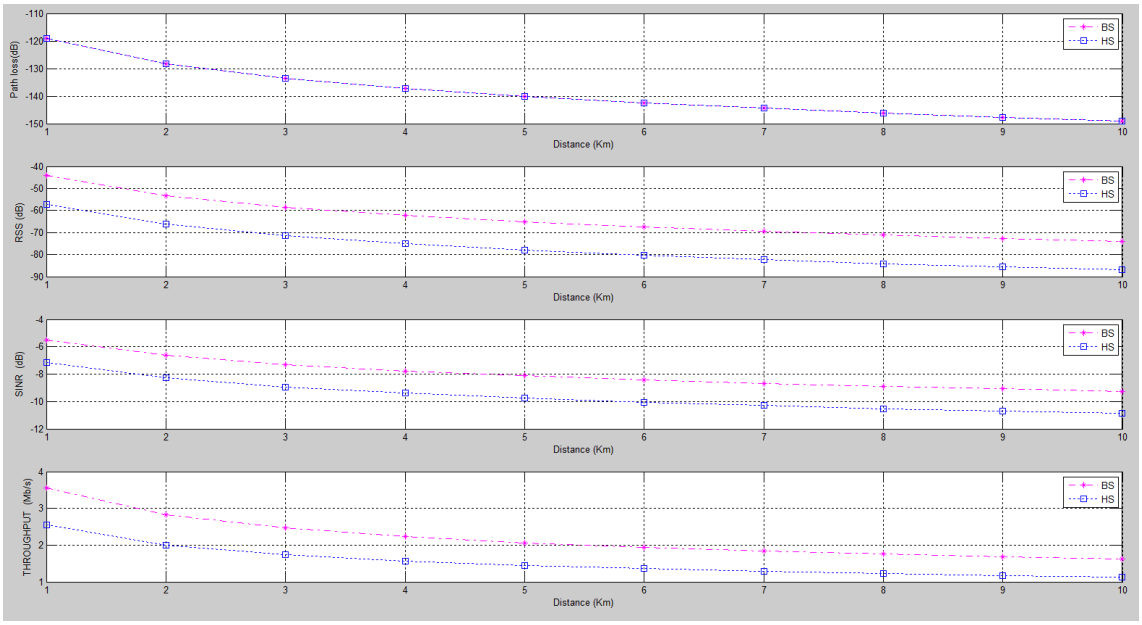

Fig. 5: Prediction plots of ITU-R P.529-3 model, at 0.2km LAP altitude, in an Urban environment – BS and HS receivers

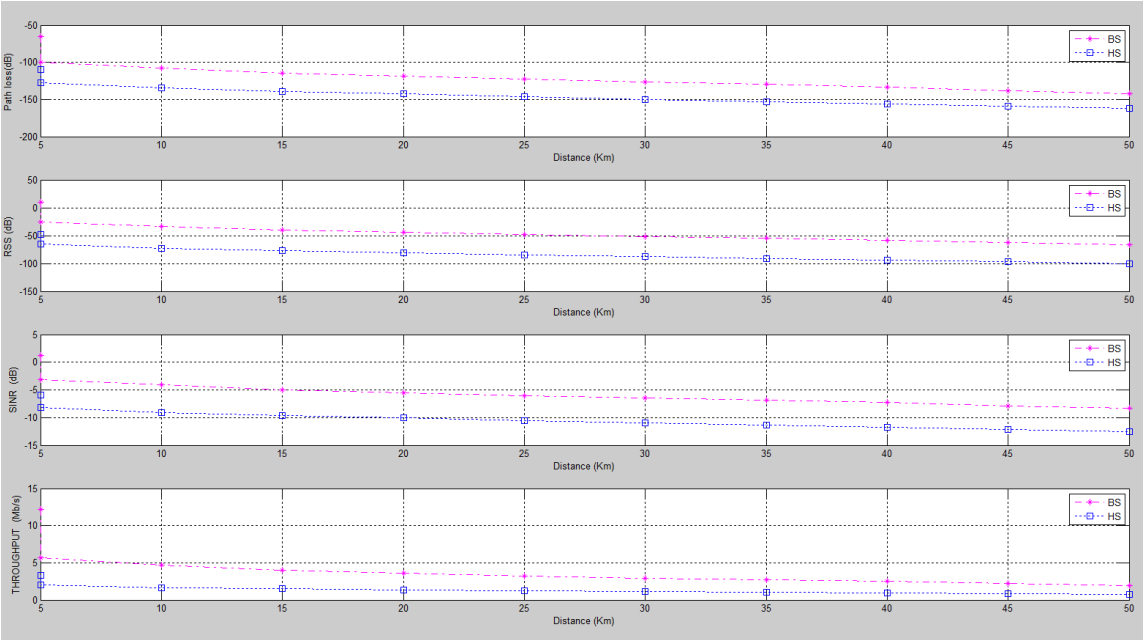

Fig. 6: Prediction plots of Okumura model, at 1km LAP altitude, in an Urban environment – BS and HS receivers

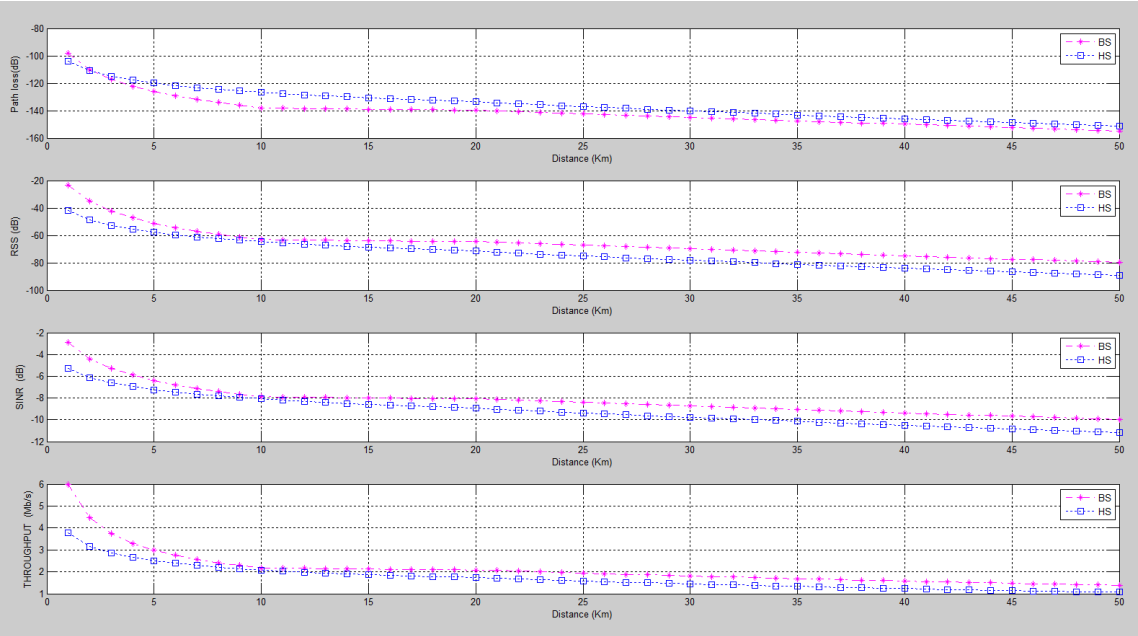

Fig. 7: Prediction plots of Hata-Davidson model, at 2.5km LAP altitude, in an Urban environment – BS and HS receivers

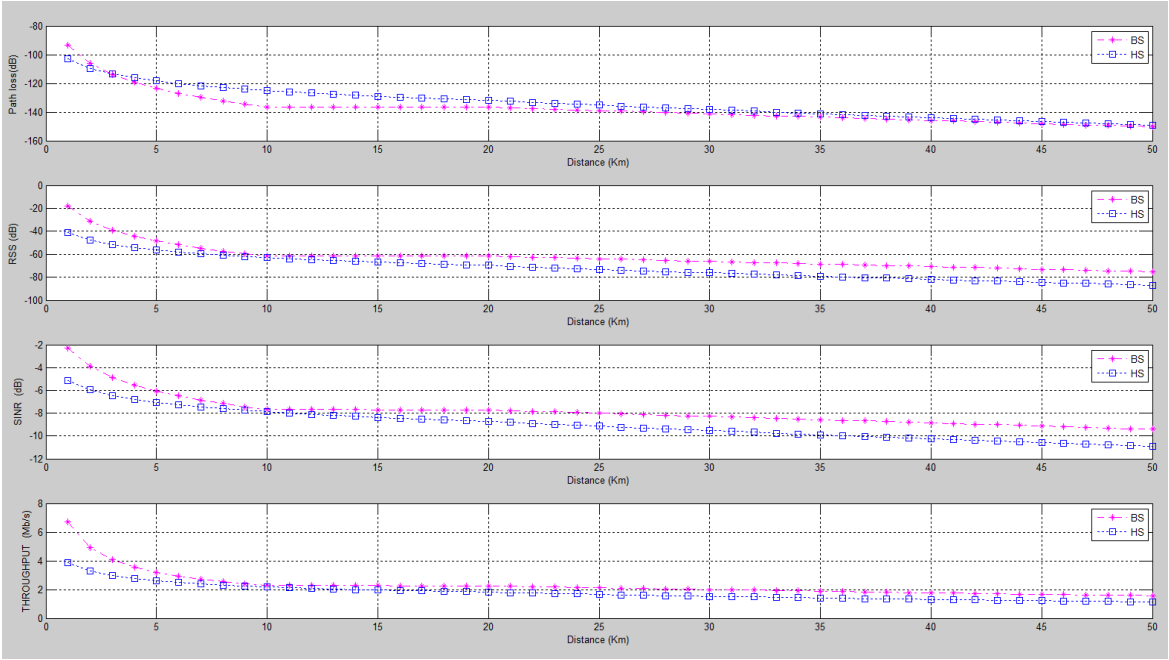

Fig. 8: Prediction plots of ATG model, at 5km LAP altitude, in an Urban environment – BS and HS receivers

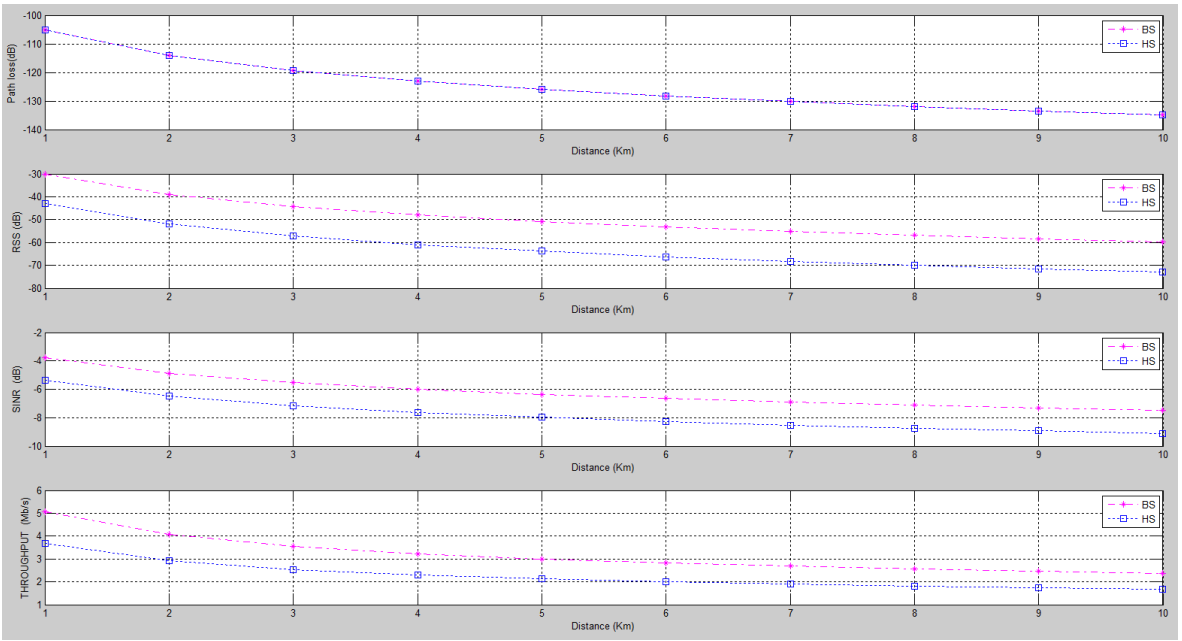

Fig. 9: Prediction plots of ITU-R P.529-3 model, at 0.2km LAP altitude, in a Suburban environment – BS and HS receivers

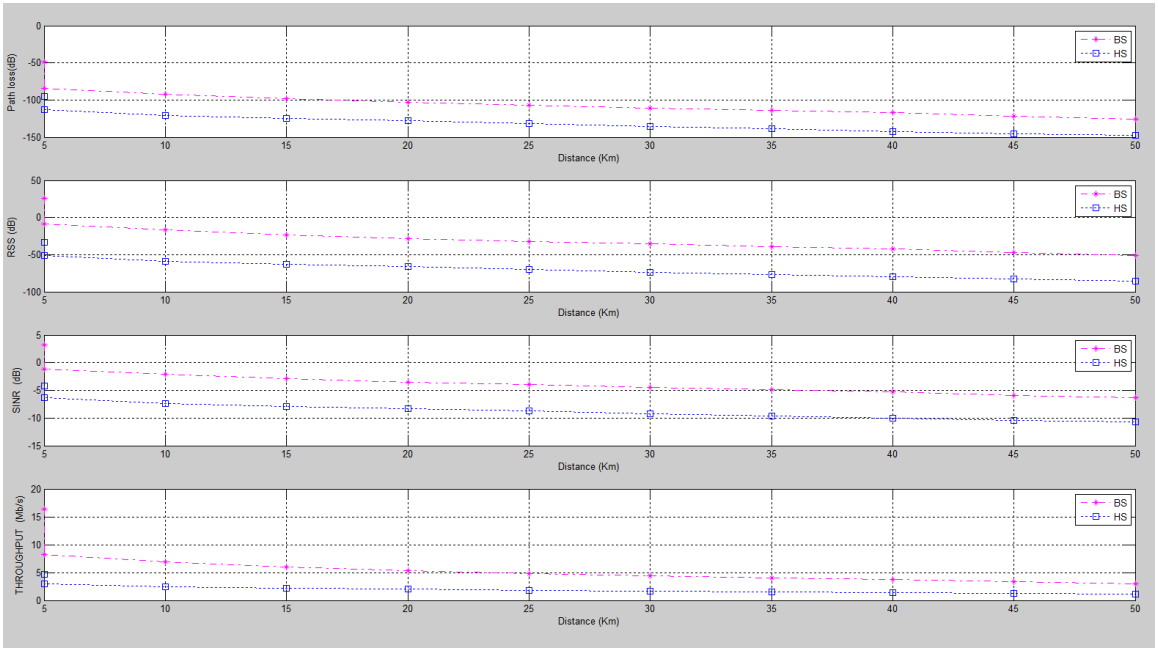

Fig. 10: Prediction plots of Okumura model, at 1km LAP altitude, in a Suburban environment – BS and HS receivers

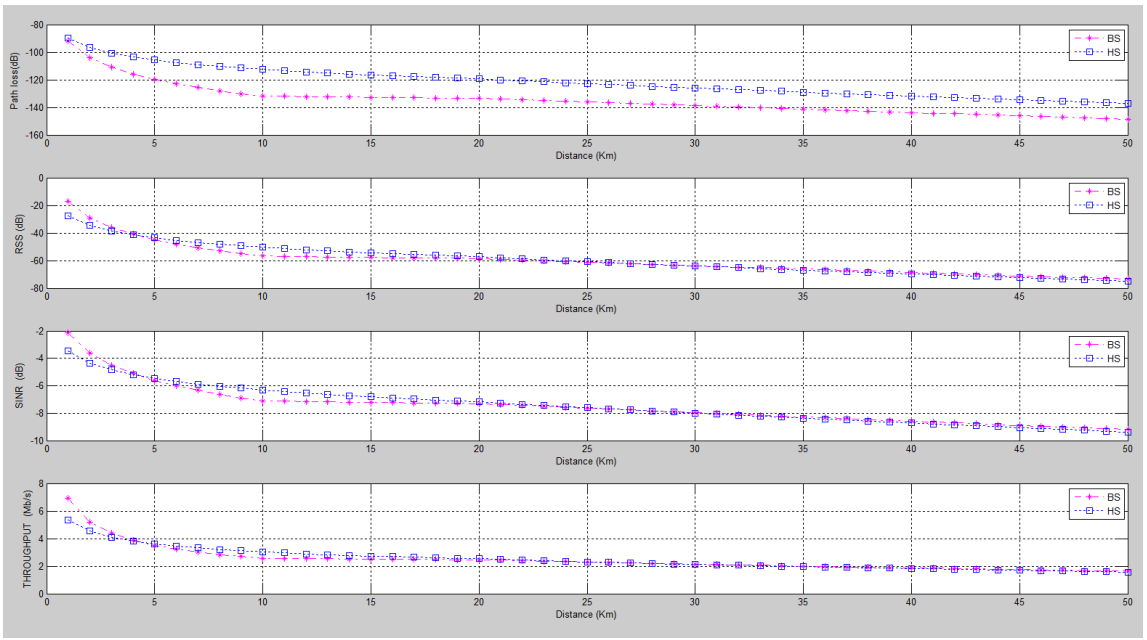

Fig. 11: Prediction plots of Hata-Davidson model, at 2.5km LAP altitude, in a Suburban environment – BS and HS receivers

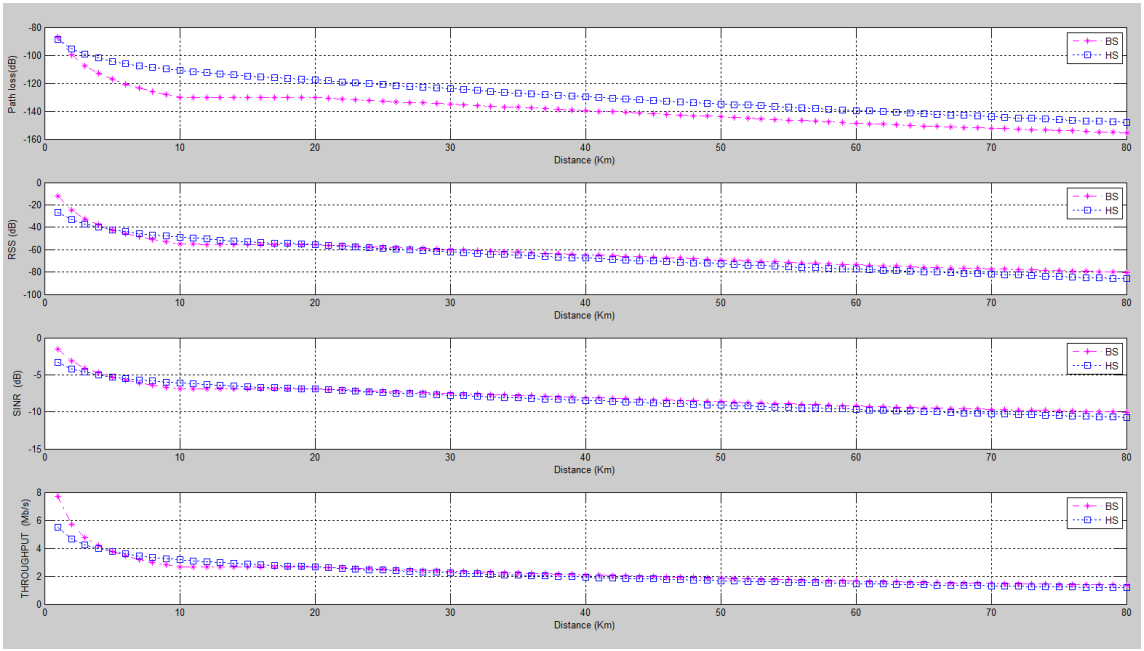

Fig. 12: Prediction plots of ATG model, at 5km LAP altitude, in a Suburban environment – BS and HS receivers

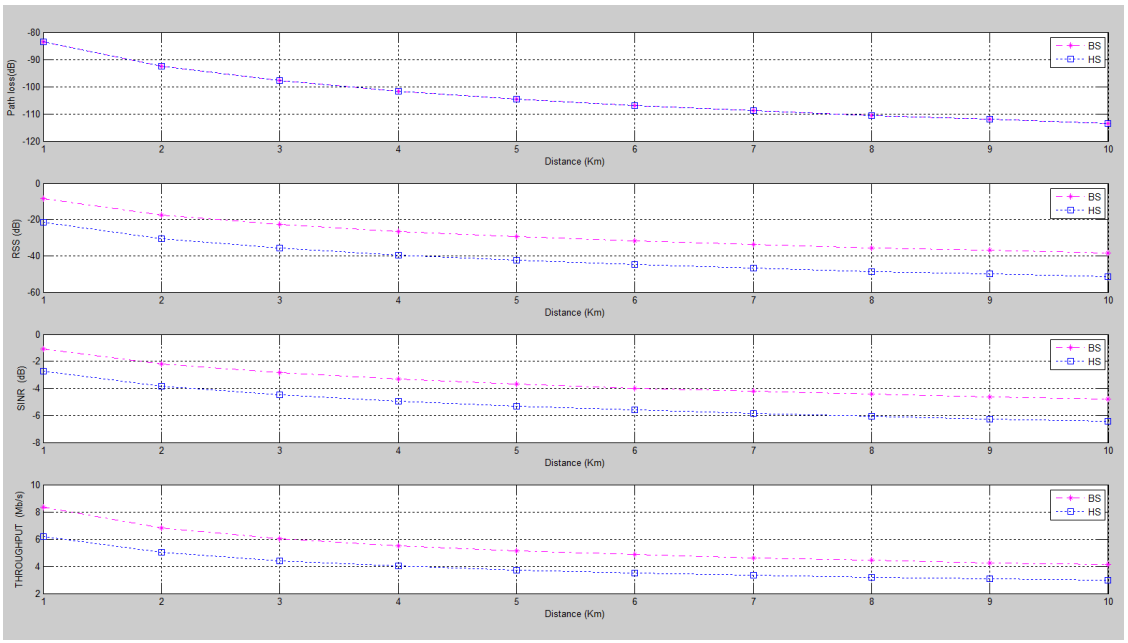

Fig. 13: Prediction plots of ITU-R P.529-3 model, at 0.2km LAP altitude, in a Rural environment – BS and HS receivers

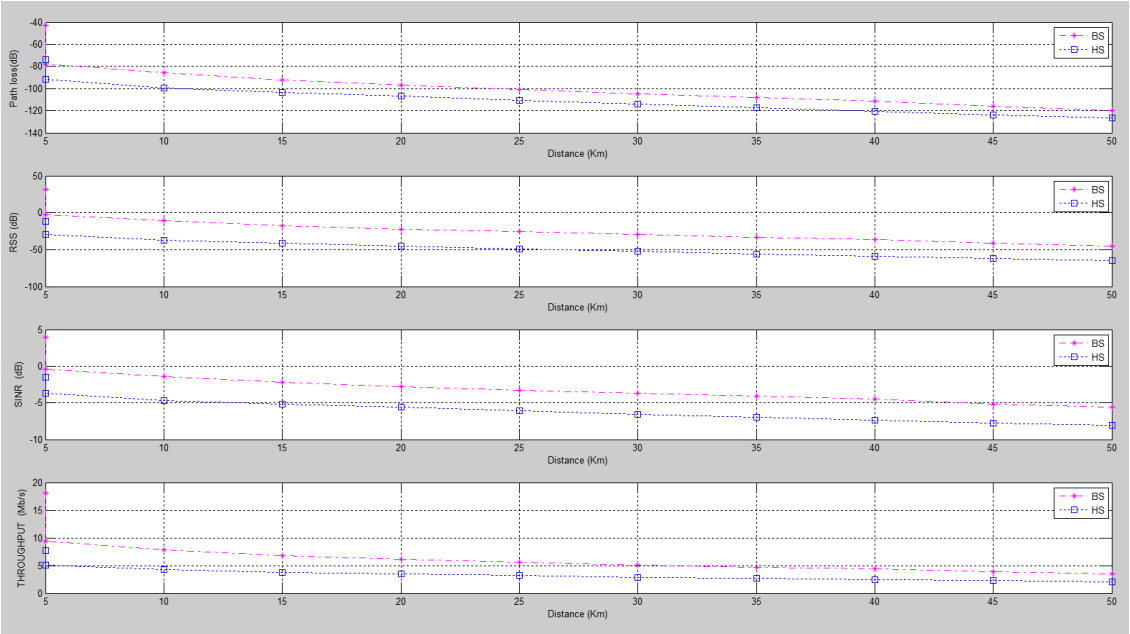

Fig. 14: Prediction plots of Okumura model, at 1km LAP altitude, in a Rural environment – BS and HS receivers

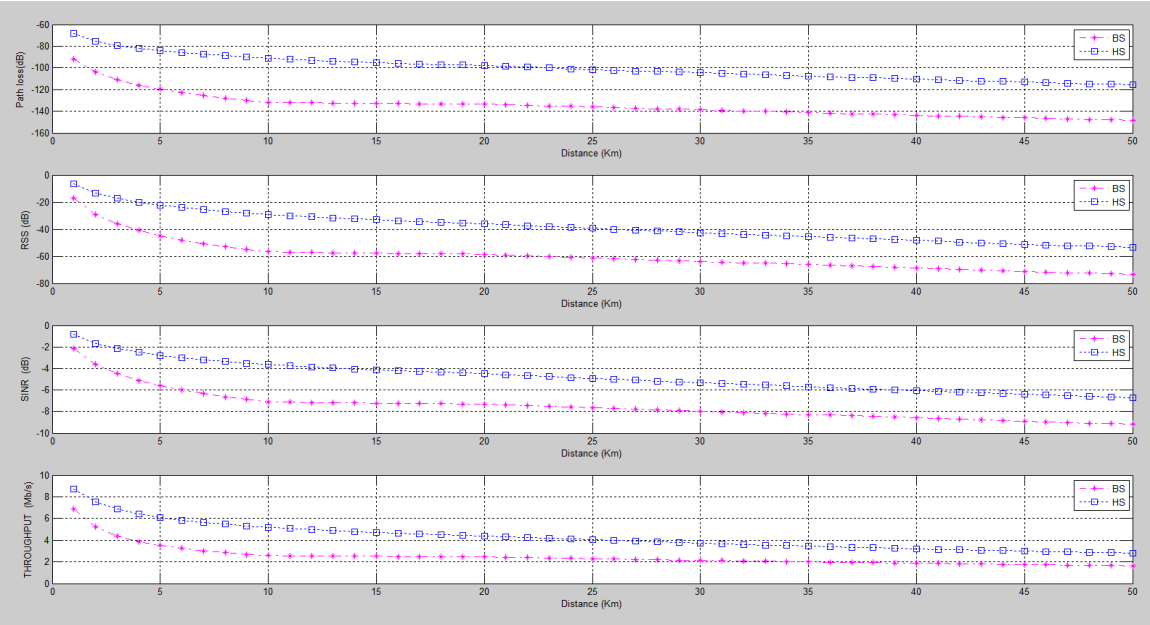

Fig. 15: Prediction plots of Hata-Davidson model, at 2.5km LAP altitude, in a Rural environment – BS and HS receivers

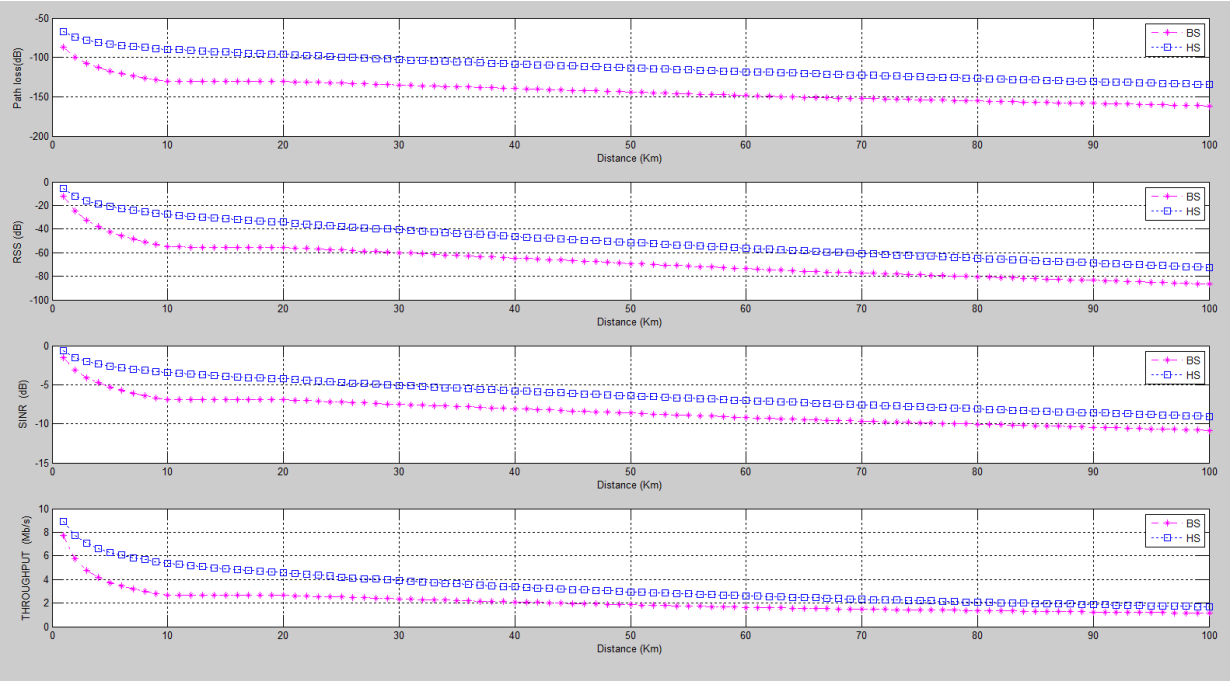

Fig. 16: Prediction plots of ATG model, at 5km LAP altitude, in a Rural environment – BS and HS receivers

4 EVOLUTION OF AN OPTIMAL PROPAGATION MODEL

The machine learning technique deployed for evolution of an optimal propagation model is Neural Nets' (NNs) Self-Organizing Map (SOM) alongside its NNs Feedback Forward fitting tool, as Fig.17 below illustrates.

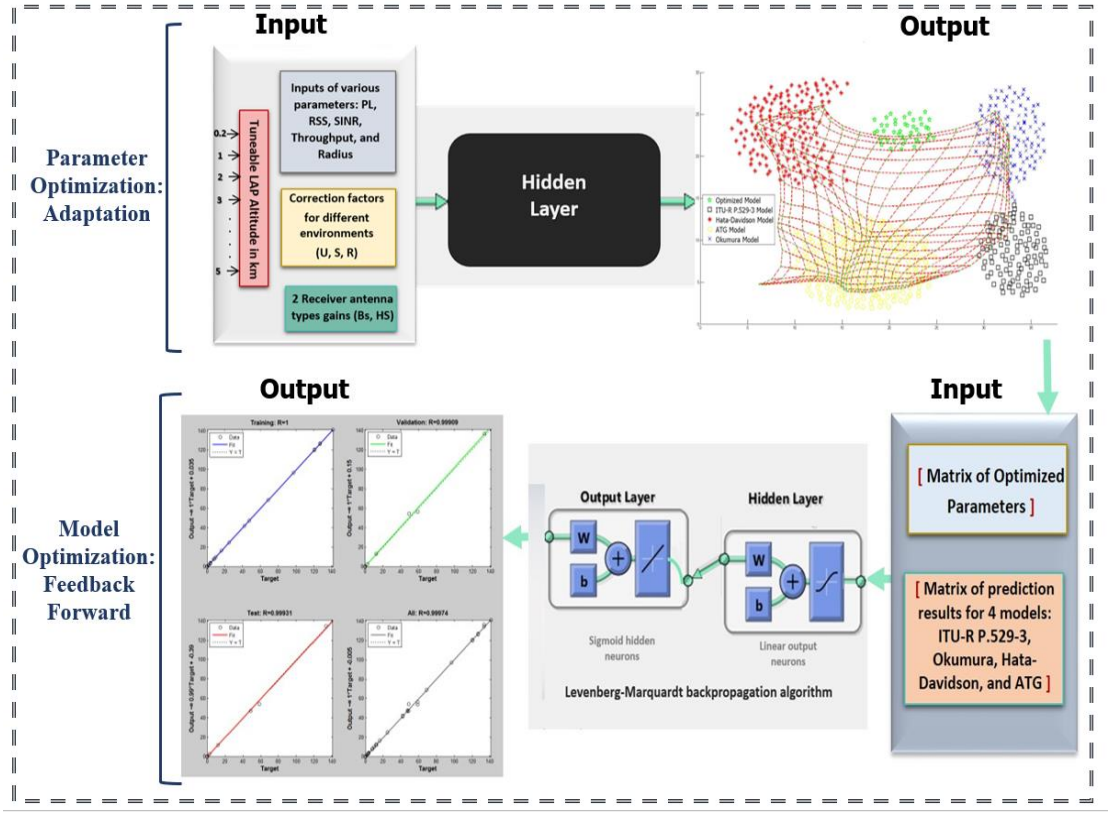

Fig.17: Machine Learning Optimization Framework using Neural Nets

The first step in optimization deploys a minimax technique at several LAP altitudes across urban, suburban, and rural environments to optimize the PL, RSS, SINR, Throughput, and Radius. The second step in optimization deploys the Levenberg-Marquardt backpropagation algorithm using the NNs Feedback Forward fitting tool to evaluate the performance of the optimized set of parameters with the four simulated models.

The application of NNs commences with its training with sample input data that produces a 2D discrete representation of the input space, the map, through the SOM's pattern recognition and clustering and thereby enabling it to predict optimal output values based on three basic components of a neuron: synaptic weights, summing function, and activation function. Usually, the SOM has a 2D lattice of neurons and each neuron is considered as a cluster [74-77]. The SOM algorithm runs over two phases: Learning and Adaptive.

4.1 Learning Phase

The learning phase commences with initializing, as per equation 28, each neuron's weight, w_i, with a random value between 0 and 1, the learning rate $\eta(n)$, to 1, and the maximum number of iterations, $n\,max$, to 1000. $\eta(n)$ is a training parameter that controls the size of the weight vector in learning of SOM.

$$w_1 = [w_{j1} \dots \dots w_{jm}]\mathrm{T} \tag{28}$$
$$\eta(n) = 1, \quad n\,max = 1000$$

We adopt an unsupervised NN approach which is typical of Kohonen's NN-SOM, for which no labelled training data is required during the learning process. Instead it learns from input data [76]. Following initialization, a stimulus, i.e. a random representative input sample from the data set, **x**, is presented to the network for training, as per equation 29.

$$x = [x_1 \dots \dots x_m]\mathrm{T} \tag{29}$$

All inputs (**x**) used for training the network are sourced from a training data set. PL varies from the lowest value to the MAPL threshold of -146.5dB and -133.5dB for BS and HS respectively. RSS varies from the lowest value to WiMAX threshold of -91dBm, SINR ranges between 4dBi and 19dBi, Throughput ranges between 1 and 10, and Radius ranges between 1 and 100km. The learning phase then proceeds with the definition of the topological map, M_A, using a lattice of neurons, A, as per equation 30.

$$\mathrm{M}_A = \begin{cases} \Psi_{A\to X} : X \to A; & x \in X \to s(x) \in A \\ \Psi_{X\to A} : A \to X; & i \in A \to w_i \in X_i \end{cases} \tag{30}$$

The map, $\mathrm{M}_A = \Psi_{A\to X}, \Psi_{X\to A}$, defines concurrently two mappings, from an input vector $x \in X$ to a neuron i $\in A$, and an inverse mapping from neuron $i \in A$ to a weight vector $w_i \in X$. Finally, with each input pattern all neurons attempt to compute the Best Matching Unit (BMU) by calculating the Euclidean distance between the input vector and the weights of each neuron. The shortest distance between a matching winning neuron and the input data x is declared as the BMU as per equation 31, where m denotes the dimension of the input pattern, $d_{j,i}$ denotes the distance between two neurons i and j and $h_{j,i}$ denotes a function of topological neighbourhood to measure how close the neurons i and j are.

$$d_{w,x} = \sqrt{\sum_{m=1}^{n} \left(x_m - w_{jm}\right)^2} \tag{31}$$

4.2 Adaptive Phase

The adaptive phase involves updating of synaptic weight vectors of winning neuron and neighbours as per equations 32 and 33, where σ is the effective width of the neighborhood which decreases with each iteration, σ_0 is the initial value of σ, and $\boldsymbol{\tau}$ is the time constant defining the slope of the graph. The winner neuron updates itself and its neighbour neurons with the patterns of the input dataset using synaptic weight adjustments as per equation 34, where $w_j(n)$ stops the weight from going to infinity. Topological ordering of clusters to detect rapidly both different and similar clusters gets underway and over the course of this phase, the algorithm converges to the most suitable clusters. The neighbourhood function is a Gaussian.

In equation 35 each minimax parameter is optimized through its updated synaptic weight $w_j(n+1)$, whereby it attempts to optimize the values of the vector; minimizing PL, maintaining SINR, and maximizing RSS, Throughput, and Radius. Throughput which refers to the average rate of data that be transmitted successfully

over a set period of time through a communication channel, is one of performance indicators that decreases with path loss, distance, and shadowing. M_j refers to each of the four propagation models and M_{opt} refers to optimized model at each altitude at a specific environment. After each cycle, the parameters are recomputed, and new vectors are put on the converged map. Min <> Max denotes the lower and upper bound values respectively of a floating parameter. An example of this is maintaining SINR between 4dBi and 20dBi. The process is repeated through equations 28-35 up to the maximum number of iterations (n), or no significant change in the map has occurred.

$$h_{j,i} = exp(\frac{-{d_{j,i}}^2}{2\sigma^2}) \quad (32)$$

$$\sigma(n) = \sigma_0 exp^{(\frac{-n}{\tau})} \ , \quad \sigma_0 = 5 \quad (33)$$

$$w_j(n+1) = w_j(n) + \eta(n)\, h_{j,i(x)}(n)(x - w_j(n)) \quad (34)$$

$$M_{opt} = [w_j(n+1) * \mathrm{Mj_{min}}\ (\mathrm{PL}),\ w_j(n+1) * \mathrm{Mj_{max}}\ (\mathrm{RSS}),\ w_j(n+1) * \mathrm{Mj_{min<>max}}\ (\mathrm{SINR}),\ w_j(n+1) * \mathrm{Mj_{max}}\ (\mathrm{Throughput}),\ w_j(n+1) * \mathrm{Mj_{max}}\ (\mathrm{Radius})] \quad (35)$$

The NN fitting tool in MATLAB supports data selection, network creation and training, and network performance evaluation using Mean Square Error (MSE) and regression analysis. The NN design of a two-layer feedforward network consists of one hidden layer using a tan-sigmoid transfer function, and a linear neuron output layer. This enables the network to learn of nonlinear and linear relations between input and output vectors. The linear transfer function, however, to the tan-sigmoid function, allows the network to produce values outside the -1 to + 1 range. NN suits multi-dimensional plotting problems well, given reliable data and adequate neurons in its hidden layer. Adjusting weights and biases during training of a network are considered to minimize a network performance function that uses the MSE, the correlation and average squared error between the network outputs and target outputs. Another design decision is the choice of the training function. The Levenberg-Marquardt algorithm uses the Hessian matrix approximation of Newton's method, which is regarded as faster and more accurate near an error minimum. Thus, the scalar $\boldsymbol{\mu}$ decreases after each drop-in performance function, which means the performance function is continuously reduced at each iteration of the algorithm [75, 78-79].

The Hessian matrix can be approximated as:

$$H = JTJ \quad (36)$$

The gradient is calculated as:

$$g = JT_e \quad (37)$$

The Hessian matrix approximation of Newton's method is as:

$$xk + 1 = xk - [JTJ + \mu J] - 1JT_e \quad (38)$$

where J is a Jacobian matrix which consists of first values of the network errors in consideration of the assigned weights and biases and e is a vector of network errors. The Jacobian matrix can be computed via a backpropagation technique that is less complex than the Hessian matrix. The available input vectors and target vectors will be randomly divided into three sets: *Training* makes offerings to the network while training, and the network is tuned in response to its error, hence, calculating the gradient and updating the weights and biases, *Validation* which measures network generalization and stops training when generalization halts improving and *Testing* which delivers an autonomous measure of performance during and after training, thus with no effect on training.

Equations (28) through to (35) are simulated in MATLAB under the same conditions. PL is kept as low as possible to achieve a certain level of reception with the smallest attenuated signal not exceeding the MAPL, i.e. between -146.5dB and -133.5dB for BS and HS respectively. SINR is maintained between 4dBi and 19dBi. RSS is kept as high as possible to achieve a wider wireless connectivity, and to avoid service degradation and/or interruption. A threshold for RSS and SINR for both BS and HS antennas depends on modulation methods and receiver sensitivity as in the WiMAX link budget specification of Table 2. The maximum RSS value is kept between -85dBm and -91dBm [69, 80]. Throughput and coverage radius are kept as high as possible for higher data rates and wider connectivity. Fig. 18 through to Fig. 23 show an optimal set of parameters obtained across

three terrains (U, S, R) for both BS and HS antennas. The X and Y axes on Fig. 18 through to Fig. 23 represent respectively the number of rows and columns of the SOM.

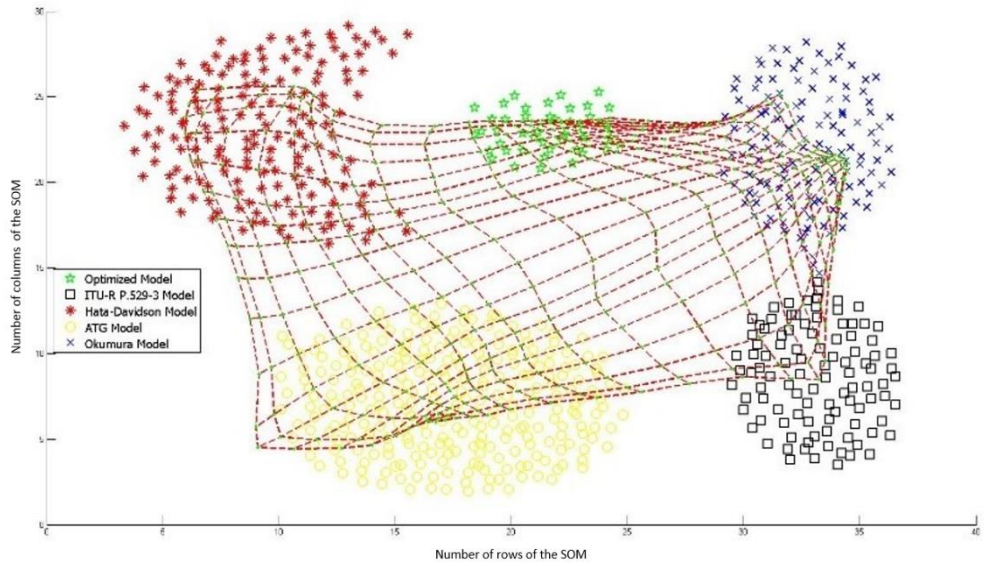

Fig. 18: Parameter optimization in an Urban Terrain – BS

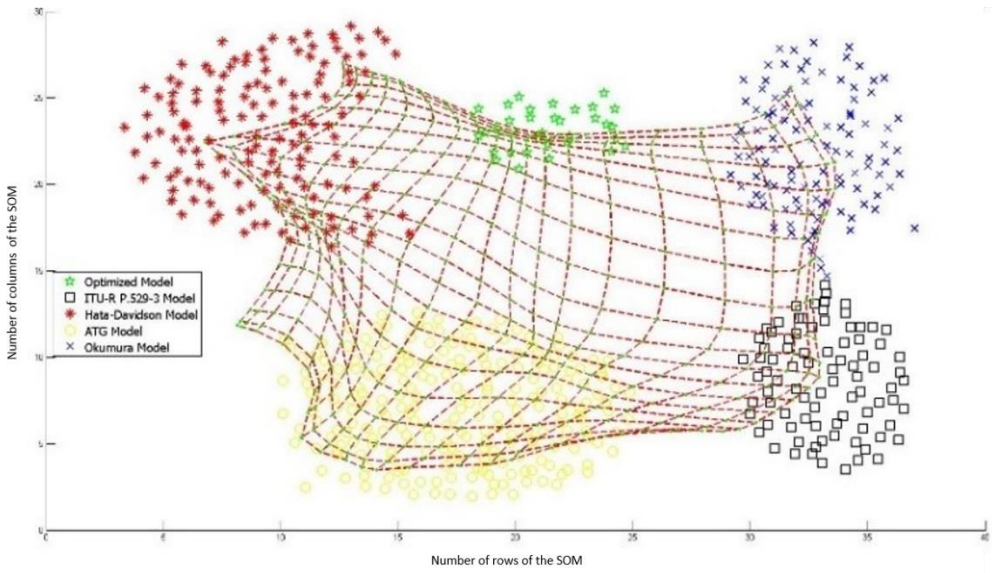

Fig. 19: Parameter optimization in an Urban Terrain – HS

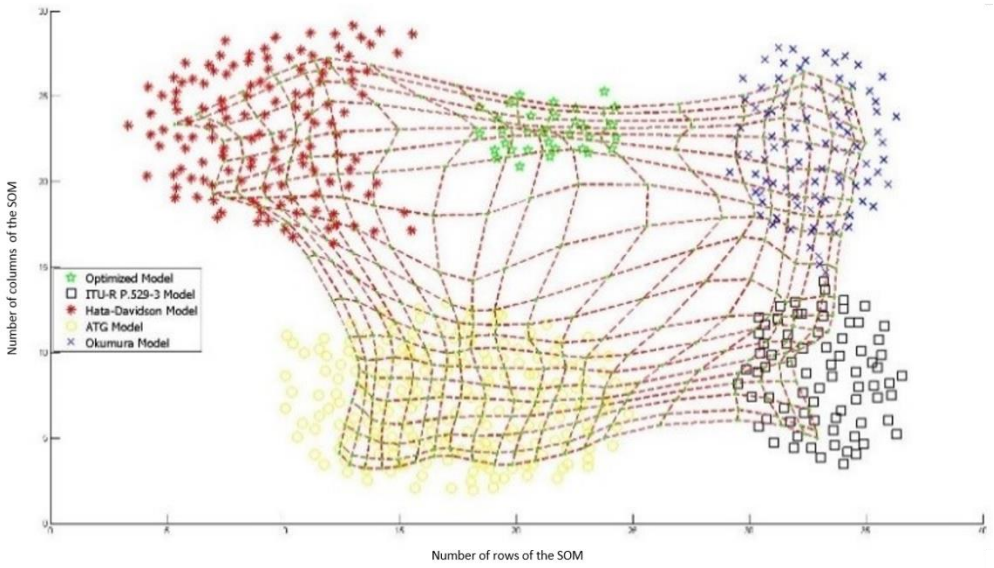

Fig. 20: Parameter optimization in a Suburban Terrain – BS

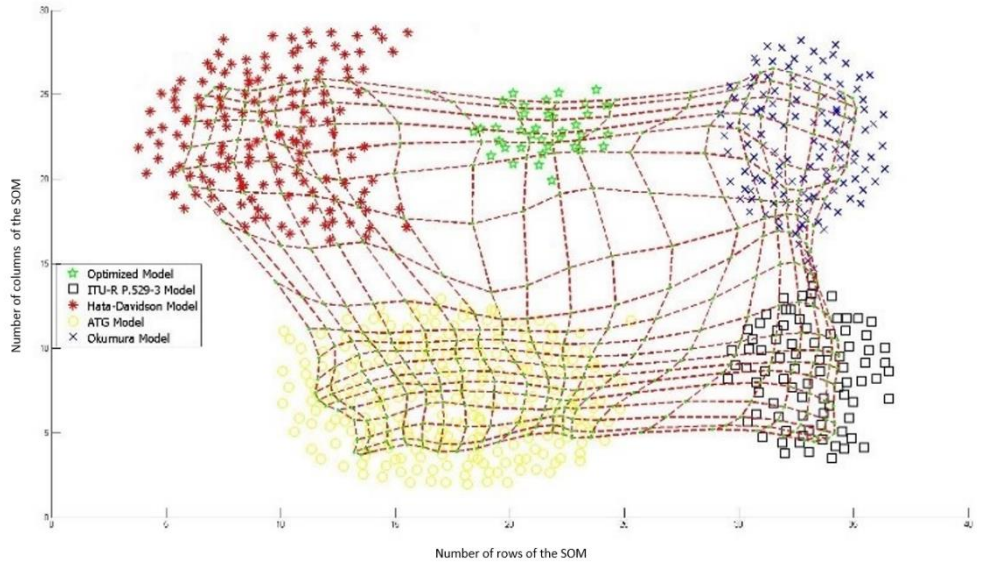

Fig. 21: Parameter optimization in a Suburban Terrain – HS

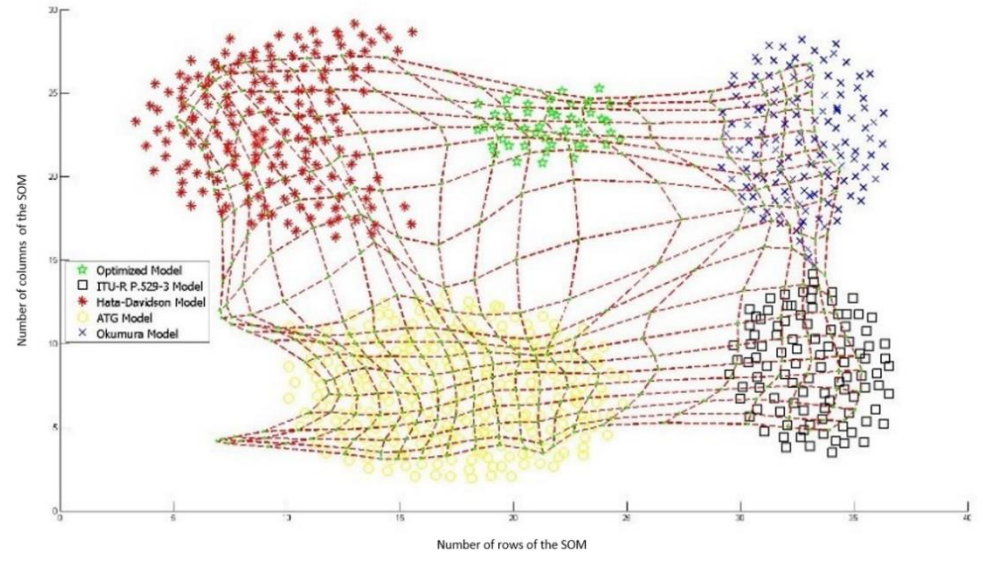

Fig. 22: Parameter optimization in a Rural Terrain – BS

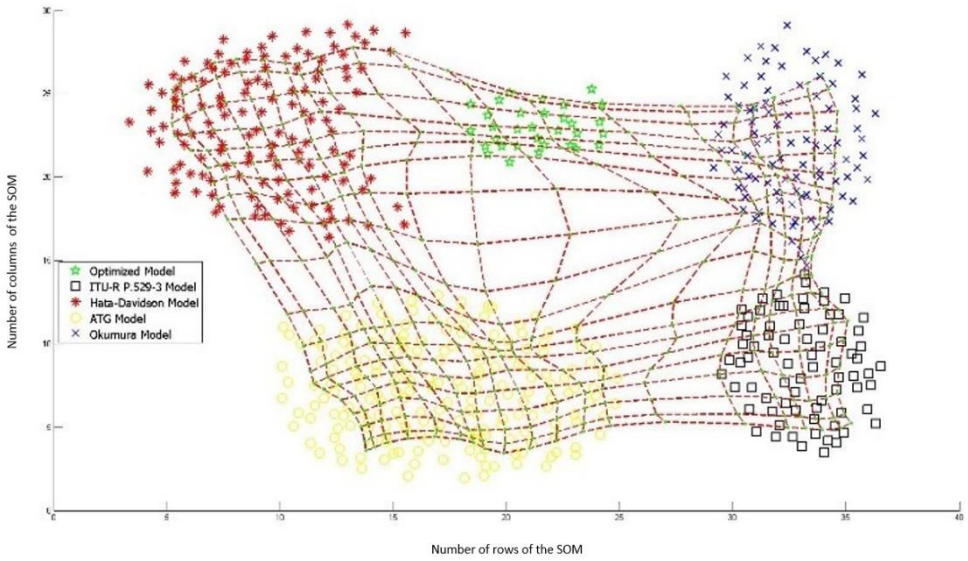

Fig. 23: Parameter optimization in a Rural Terrain – HS

After several cycles, the percentage of Training, Validation, and Testing is set at 70, 15, and 15, respectively, with the optimum number of hidden layers that yields best performance and regression being 10. The aim is not to define an optimum number of neurons, but to see if this kind of network can represent a solution. Assigning different number of neurons to the hidden layer obtains an approximation of how this impacts network performance. Small networks are trained easier, generalized better, and fewer training pairs are needed. The input vector, [96x5], is sourced from Fig. 5 through to Fig. 16. The target vector, [24x5], is sourced from Fig. 18 through to Fig. 23. A training simulation was carried out in MATLAB and results are shown on Fig. 24 through to Fig. 26.

Fig. 24 depicts how the error function minimizes during training. Batch training is carried out and completed when all training sets are input through the learning algorithm in one epoch, i.e. the maximum number of iterations, before weights get updated. The process determines the optimal number of iterations during which validation produces a minimal value. Validation uses regression plotting to determine that value. The performance is changed after each iteration of the training algorithm. This training set and validation set decreases continuously to the point where overfitting happens. The network is trained for 18 epochs (iterations). After the 12th epoch the validation performance starts to increase to satisfy the condition of exhibiting an acceptable performance. After seven validation checks the network stops its training and returns to the state where the minimum validation performance is observed as indicated by the green circle. The result is fitting because, firstly, the final MSE is small, secondly, the test and validation set errors have similar characteristics, thirdly, no significant overfitting occurs before iteration 12 after which best validation performance occurs.

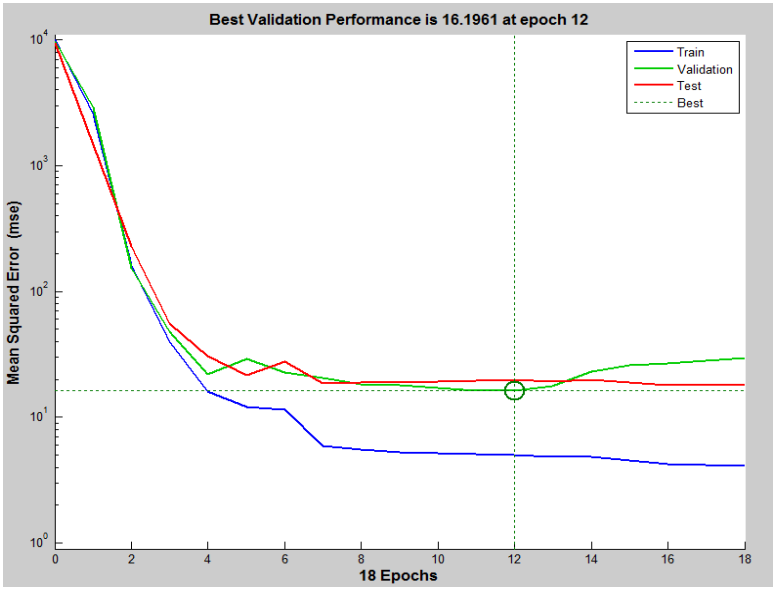

Fig. 24: Training performance

The next step in validating is to create a regression plot of outputs in relation to the targets. Fig. 25 plots targets against training, validation, and test sets, where Y and T stand respectively for output and target. Perfect fit means the data should fall along a 45-degree line, where the network outputs are equal to the targets. The dashed lines represent the targets which are equal to the difference between the perfect results and the outputs. The solid line indicates the best fit linear regression line between targets and outputs. The R value is a correlation coefficient and indicates the relationship between the outputs and targets. If R = 1, then there is an exact linear relationship between the two vectors. If R is close to zero, then there is no such linear relationship. For this NN, the fit is good for most of the data sets, with R values in each case at 0.99 and above. Overall, the R values are satisfactory and represent the best levels of fitness.

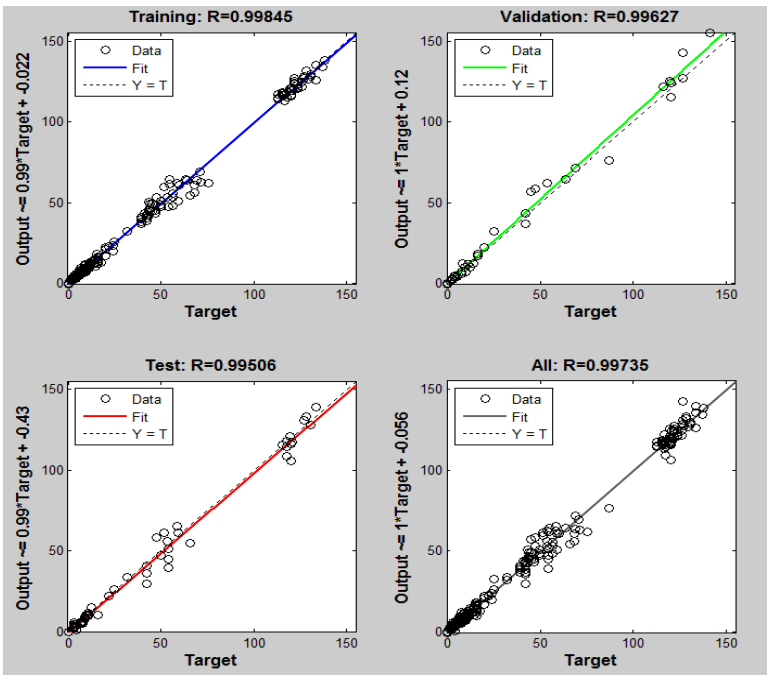

Fig. 25: Regression plots

The error histogram gives an additional verification of network performance, as Fig. 26 shows. The blue, green and red bars indicate training data, validation data and testing data, respectively. The largest part of data fall on the zero-error line, which requires further examination of the outliers to decide if the data is correct, or if those data points are disparate than the rest of the data set. If it is the former, then the network is generalizing these

points, which is exactly the case with ours. It can be observed that the dataset distribution nears zero with only a few exceptions for the log sigmoid and tan sigmoid activation function. Therefore, as the figure shows the data fitting errors are distributed within a reasonably good range around zero.

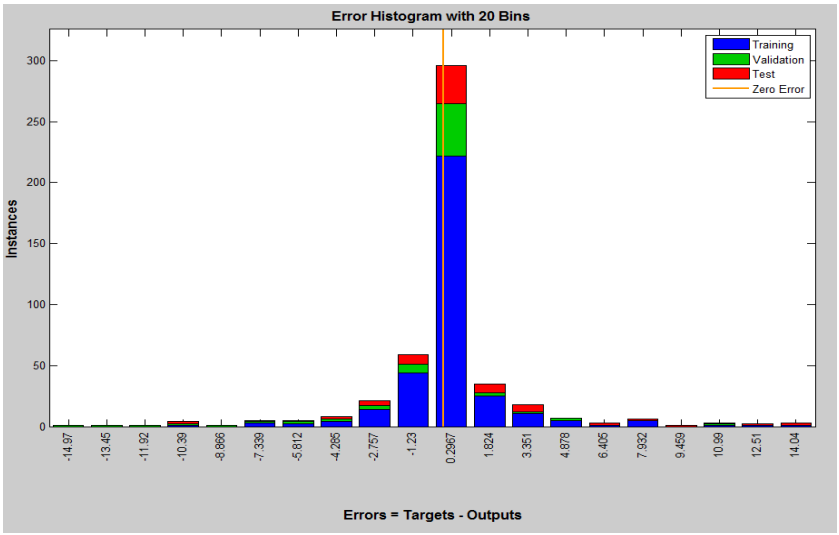

Fig. 26: Error Histogram plot for Training data

Overall, R values are fitting and represent best fitness levels. Therefore, the NN optimized models deliver reasonable prediction results. Overfitting might happen during the training of the NN, which is undesirable, thus the MSE on the training set is already at a small value, so that is a reasonable indicator.

5 COMPARATIVE EVALUATION

This section compares the prediction results generated by both the optimised and the non-optimised propagation models via MATLAB software. This method has provided further opportunities for data interpretation and validation of the optimised propagation model. Numerical prediction results of the both optimized and non-optimized models are shown on Fig. 27 through to Fig. 32. M1, M2, M3, and M4 denote ITU-R P.529-3, Okumura, Hata-Davidson, and ATG models respectively.

Optimised PL values float between -94.68dB and -136.28dB across all three environments with an improvement average between 4% to 15% in comparison to those of the four models. The optimised PL is also below the MAPL for BS and HS antennas across all environments. The optimised RSS achieves better predictions in comparison to ITU-R P.529-3, Hata-Davidson, and ATG models by an average of 3% through to 27%. However, the Okumura model tops for the highest RSS value. The RSS for the HS antenna is less than the value of BS because of the antenna gain values. Unsurprisingly, increasing transmitter altitude or transmission power, increases both the coverage area and RSS. Keeping transmission power constant at different transmitter altitudes yields varying levels of RSS. Optimised SINR is kept within the acceptable average of 5.17dB and 10.91dB, with values below 4dB deemed unacceptable and considered inadequate, while any values above 19dBi are regarded as wasted transmitter power. SINR values in BS are higher than those in HS across all environments and altitudes due to achieved RSS results. Optimised throughput yields an improved predicted result between 2% and 10% in comparison to the four models. Throughput decreases with LAP altitudes in all terrains, and due to increases in path loss and distance, and shadowing.

The optimised radius predicts a wider wireless connectivity across the three environments with an average range between 2km and 6km. The modification that has been considered in the empirical models in calculating the coverage radius distance, i.e. the adaptation of an elevation angle, instead of the traditional approach of coverage calculation seems more suitable to LAP quasi-stationary condition. Overall, the optimised predictions show that PL is kept as low as possible to achieve a certain level of reception with the smallest attenuated signal. Radius, throughput and RSS are kept as high as possible to achieve a wider and stronger connectivity. The radius increases with transmitter altitude, as well as with changing from an urban to a rural environment, due to a

decrease in the elevation angle. In addition, the limited effect of shadowing and reflection leads to an increase in distance.

Overall, the non-optimised predictions show that PL, RSS, and SINR values increase across all models and environments as the transmitter altitude increases, due to the increase in coverage. Throughput decreases as the transmitter altitude increases. It is observed that all the considered link budget parameters are different between HS and BS due to the differences in antenna gain. The receiver antenna height is set at 1m for HS and 5m for BS which yields an advantage for the Okumura model in achieving better coverage since a receiver antenna height of over 3m yields the same result. However, as the other adapted models accommodate receiver antenna heights of up to 30m, every increase in receiver antenna height impacts their coverage range. The adaptation of an elevation angle in calculating the coverage instead of the traditional coverage calculation, and the inclusion of MIMO diversity gain techniques to improve reliability in all four adapted models yield improved predictions. The improvement is evidenced in the low PL and extended coverage range. Thus, the combined antenna and diversity gains are of importance to enhance RSS as low elevation angles leads to increase in the distance between platform and terrestrial users.

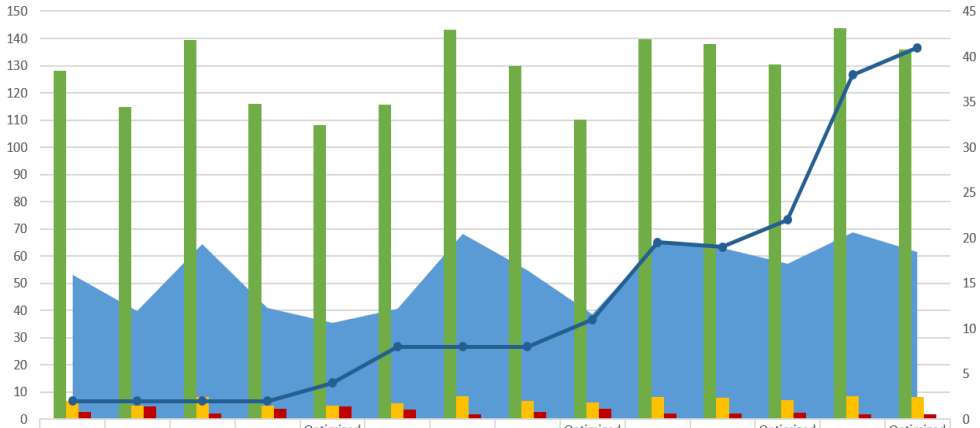

	M1_0.2km	M2_0.2km	M3_0.2km	M4_0.2km	Optimized BS_0.2km	M2_1km	M3_1km	M4_1km	Optimized BS_1km	M3_2.5km	M4_2.5km	Optimized BS_2.5km	M4_5km	Optimized BS_5km
RSS (dBm)	53.18	39.7	64.55	40.96	35.42	40.54	68.19	54.93	38.77	64.6	62.87	57.3	68.86	61.4
PL (dB)	128.18	114.7	139.55	115.96	108.11	115.54	143.19	129.93	110.23	139.6	137.87	130.53	143.86	135.83
SINR (dB)	6.65	4.97	8.07	5.12	5.17	5.94	8.52	6.87	6.11	8.07	7.86	7.18	8.61	8.21
Throughput (Mb/S)	2.83	4.65	2.09	3.87	4.78	3.7	1.96	2.7	3.86	2.09	2.19	2.34	1.86	1.95
Radius (km)	2	2	2	2	4	8	8	8	11	19.5	19	22	38	41

Fig. 27: Optimised parameters in comparison to predictions with the four adapted models in an urban environment – BS

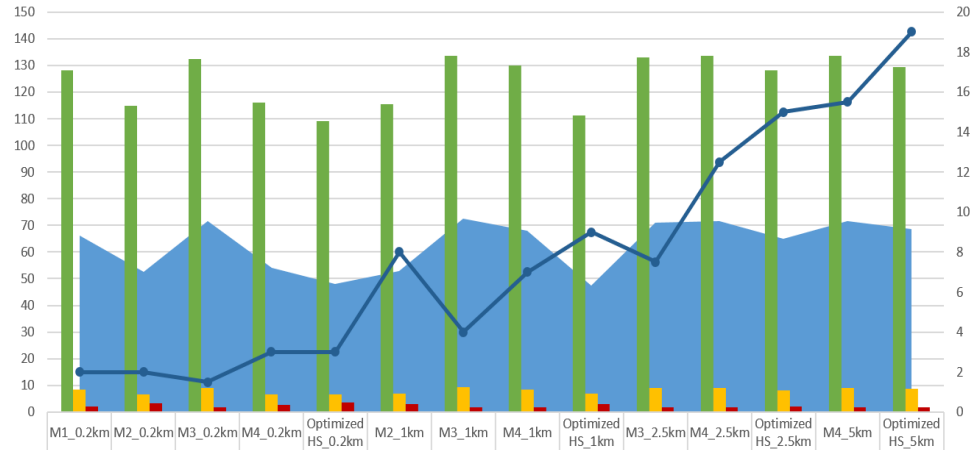

	M1_0.2km	M2_0.2km	M3_0.2km	M4_0.2km	Optimized HS_0.2km	M2_1km	M3_1km	M4_1km	Optimized HS_1km	M3_2.5km	M4_2.5km	Optimized HS_2.5km	M4_5km	Optimized HS_5km
RSS (dBm)	66.18	52.7	71.5	53.96	47.91	52.89	72.5	67.93	47.39	71.09	71.5	64.81	71.5	68.54
PL (dB)	128.18	114.7	132.5	115.96	109	115.54	133.5	129.93	111.2	133.09	133.5	128.2	133.5	129.4
SINR (dB)	8.27	6.58	9	6.74	6.54	6.89	9.2	8.49	6.97	8.89	8.95	8	8.95	8.84
Throughput (Mb/S)	2	3.13	1.71	2.77	3.46	2.87	1.63	1.91	2.93	1.75	1.72	1.92	1.7	1.77
Radius (km)	2	2	1.5	3	3	8	4	7	9	7.5	12.5	15	15.5	19

Fig.28: Optimised parameters in comparison to predictions with the four adapted models in an urban environment – HS

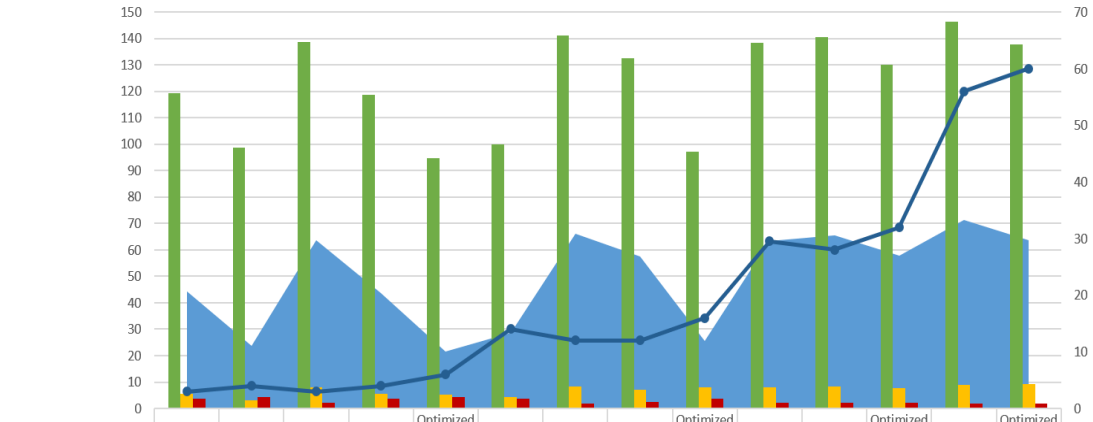

	M1_0.2km	M2_0.2km	M3_0.2km	M4_0.2km	Optimized BS_0.2km	M2_1km	M3_1km	M4_1km	Optimized BS_1km	M3_2.5km	M4_2.5km	Optimized BS_2.5km	M4_5km	Optimized BS_5km
RSS (dBm)	44.24	23.7	63.58	43.62	21.53	28.5	66.13	57.58	25.43	63.47	65.5	57.7	71.47	63.8
PL (dB)	119.24	98.7	138.58	118.62	94.68	100.03	141.13	132.58	97.1	138.47	140.5	130.16	146.47	137.89
SINR (dB)	5.53	3	7.94	5.45	5.11	4.22	8.27	7.2	8.11	7.93	8.18	7.61	8.93	9.29
Throughput (Mb/S)	3.56	4.3	2.15	3.62	4.41	3.6	2	2.52	3.81	2.15	2.04	2.29	1.74	1.87
Radius (km)	3	4	3	4	6	14	12	12	16	29.5	28	32	56	60

Fig. 29: Optimised parameters in comparison to predictions with the four adapted models in a suburban environment – BS

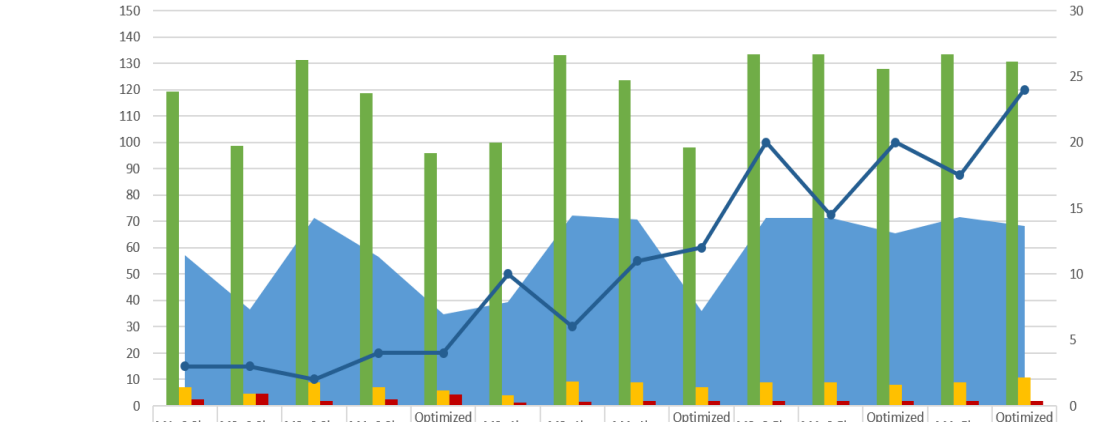

	M1_0.2km	M2_0.2km	M3_0.2km	M4_0.2km	Optimized HS_0.2km	M2_1km	M3_1km	M4_1km	Optimized HS_1km	M3_2.5km	M4_2.5km	Optimized HS_2.5km	M4_5km	Optimized HS_5km
RSS (dBm)	57.24	36.7	71.32	56.62	34.61	39.5	72.13	70.58	36.12	71.44	71.48	65.63	71.71	68.15
PL (dB)	119.24	98.7	131.32	118.62	95.91	100.03	133.13	123.58	98.06	133.44	133.48	128.01	133.5	130.66
SINR (dB)	7.15	4.59	8.91	7.07	5.86	4.05	9.15	8.82	6.96	8.93	8.93	7.91	8.96	10.74
Throughput (Mb/S)	2.54	4.65	1.74	2.58	4.38	1.08	1.64	1.78	1.94	1.74	1.73	1.86	1.69	1.69
Radius (km)	3	3	2	4	4	10	6	11	12	20	14.5	20	17.5	24

Fig.30: Optimised parameters in comparison to predictions with the four adapted models in a suburban environment – HS

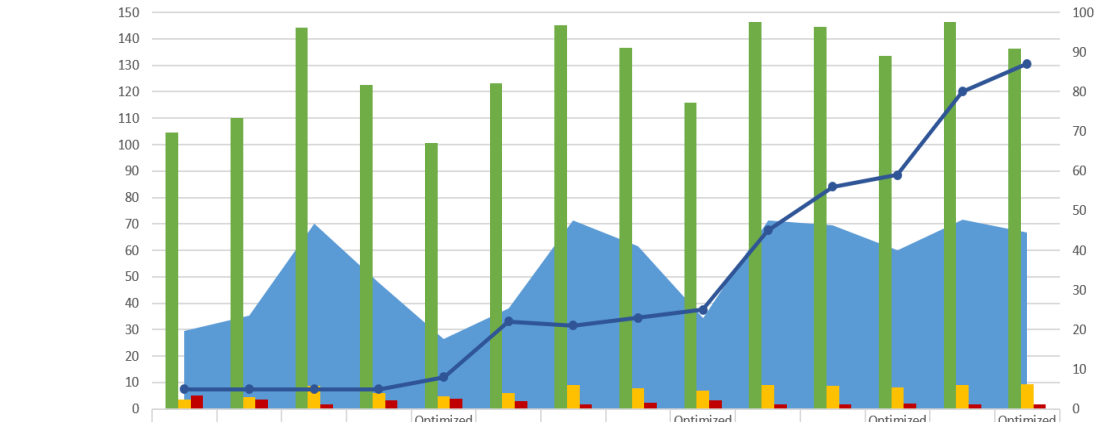

	M1_0.2km	M2_0.2km	M3_0.2km	M4_0.2km	Optimized BS_0.2km	M2_1km	M3_1km	M4_1km	Optimized BS_1km	M3_2.5km	M4_2.5km	Optimized BS_2.5km	M4_5km	Optimized BS_5km
RSS (dBm)	29.48	35.19	70.2	47.66	26.31	38.1	71.3	61.5	34.37	71.41	69.4	59.87	71.5	66.84
PL (dB)	104.48	110.19	144.2	122.66	100.68	123.1	145.3	136.5	115.83	146.41	144.4	133.42	146.5	136.28
SINR (dB)	3.68	4.39	8.74	5.96	4.65	5.85	8.99	7.69	6.78	8.93	8.67	8.24	8.92	9.5
Throughput (Mb/S)	5.14	3.47	1.8	3.2	3.87	3.01	1.62	2.26	3.34	1.74	1.83	1.95	1.7	1.81
Radius (km)	5	5	5	5	8	22	21	23	25	45	56	59	80	87

Fig. 31: Optimised parameters in comparison to predictions with the four adapted models in a rural environment – BS

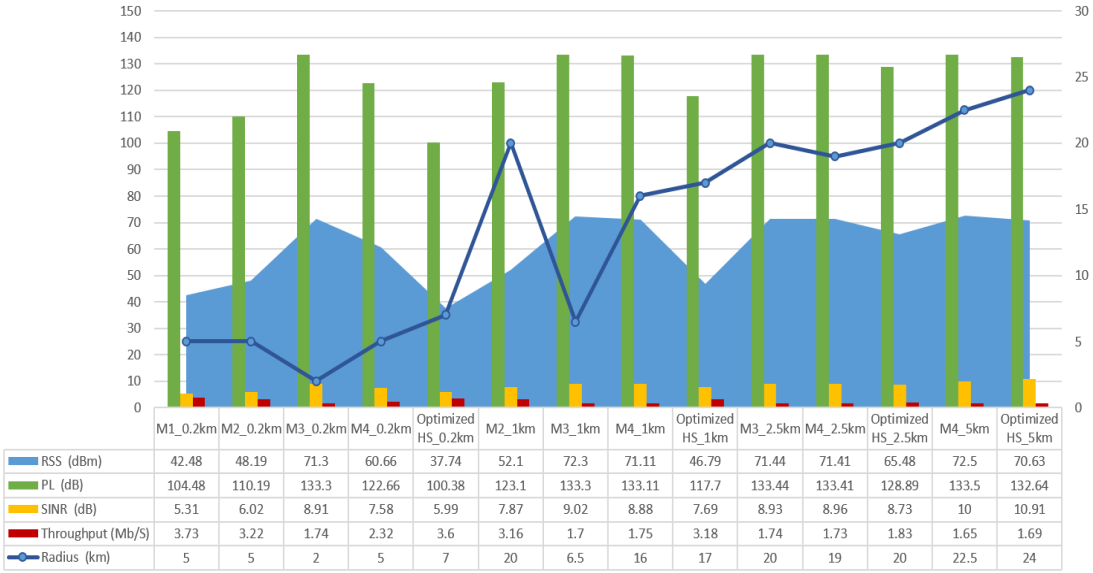

	M1_0.2km	M2_0.2km	M3_0.2km	M4_0.2km	Optimized HS_0.2km	M2_1km	M3_1km	M4_1km	Optimized HS_1km	M3_2.5km	M4_2.5km	Optimized HS_2.5km	M4_5km	Optimized HS_5km
RSS (dBm)	42.48	48.19	71.3	60.66	37.74	52.1	72.3	71.11	46.79	71.44	71.41	65.48	72.5	70.63
PL (dB)	104.48	110.19	133.3	122.66	100.38	123.1	133.3	133.11	117.7	133.44	133.41	128.89	133.5	132.64
SINR (dB)	5.31	6.02	8.91	7.58	5.99	7.87	9.02	8.88	7.69	8.93	8.96	8.73	10	10.91
Throughput (Mb/S)	3.73	3.22	1.74	2.32	3.6	3.16	1.7	1.75	3.18	1.74	1.73	1.83	1.65	1.69
Radius (km)	5	5	2	5	7	20	6.5	16	17	20	19	20	22.5	24

Fig. 32: Optimised parameters in comparison to predictions with the four adapted models in a rural environment – HS

5.1 Comparative evaluation to the four selected models following their optimisation with the Framework

In this section, we compare the performance of our optimized model to that of the four selected propagation models following their optimisation with our machine learning optimization framework in the context of a WSN in which the Eb/No and BER of an AWGN channel are assessed. Table 3 shows a matrix of the four adapted propagation models with five link budget predictions at an LAP altitude of 0.2km above ground in an urban environment and table 4 shows a matrix of our optimised propagation model with the same link budget parameters at the same altitude and in the same environment.

Table 3: The four selected propagation models after optimization with our framework

Optimized Model	**Parameters**				
	-PL (dB)	**-RSS (dBm)**	**SINR (dB)**	**Throughput (Mb/S)**	**Radius (km)**
ITU-R P.529-3	120.43	50.79	6.27	2.89	2.8
Okumura	109.67	37.88	4.94	4.7	2.5
Hata-Davidson	131.09	61.64	7.89	2.11	2.3
ATG	108.02	39.15	5.1	3.9	3.7

Table 4: Our optimised model

Model	**Parameters**				
	-PL (dB)	**-RSS (dBm)**	**SINR (dB)**	**Throughput (Mb/S)**	**Radius (km)**
NN model	108.11	35.42	5.17	4.78	4

Fig. 33 pitches the four optimised models against our optimised model, and Fig. 34 compares the five models in the context of a WSN in which the Eb/No and BER of an AWGN channel are assessed at an LAP altitude of 0.2km above ground in an urban environment. It can be observed that the optimised versions of the four models yield better results in comparison to the non-optimized versions, but our optimised model outperforms all four.

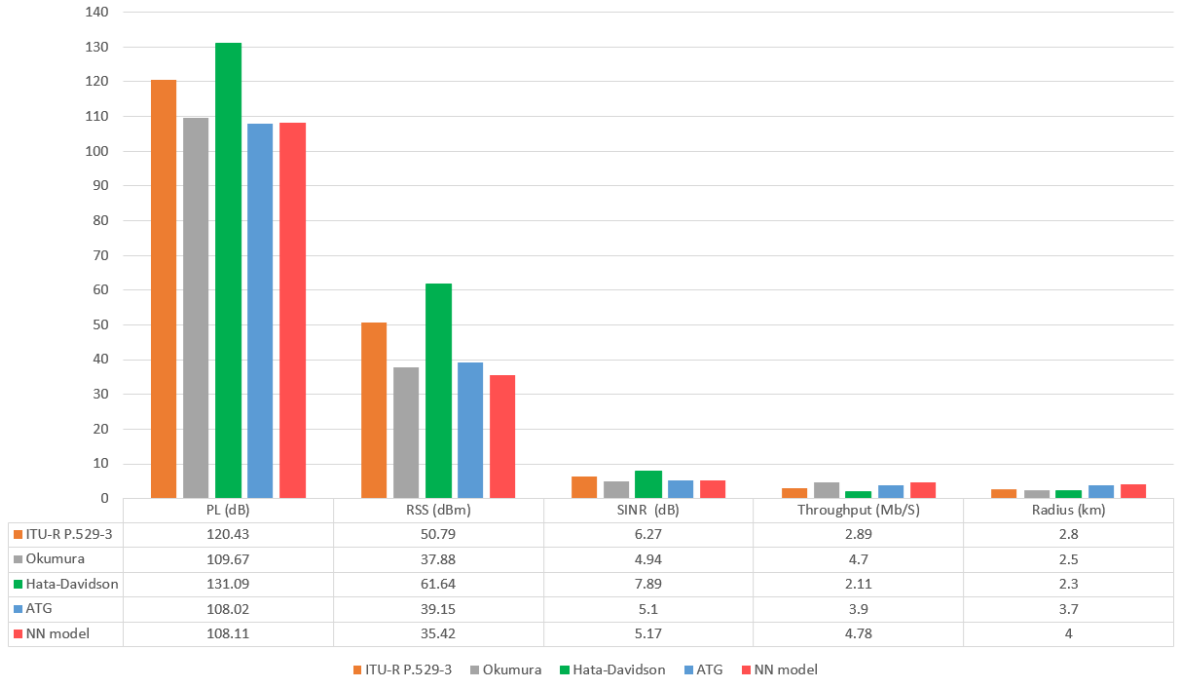

	PL (dB)	RSS (dBm)	SINR (dB)	Throughput (Mb/S)	Radius (km)
ITU-R P.529-3	120.43	50.79	6.27	2.89	2.8
Okumura	109.67	37.88	4.94	4.7	2.5
Hata-Davidson	131.09	61.64	7.89	2.11	2.3
ATG	108.02	39.15	5.1	3.9	3.7
NN model	108.11	35.42	5.17	4.78	4

Fig. 33: A parametric comparison between our optimised model and the four optimized models

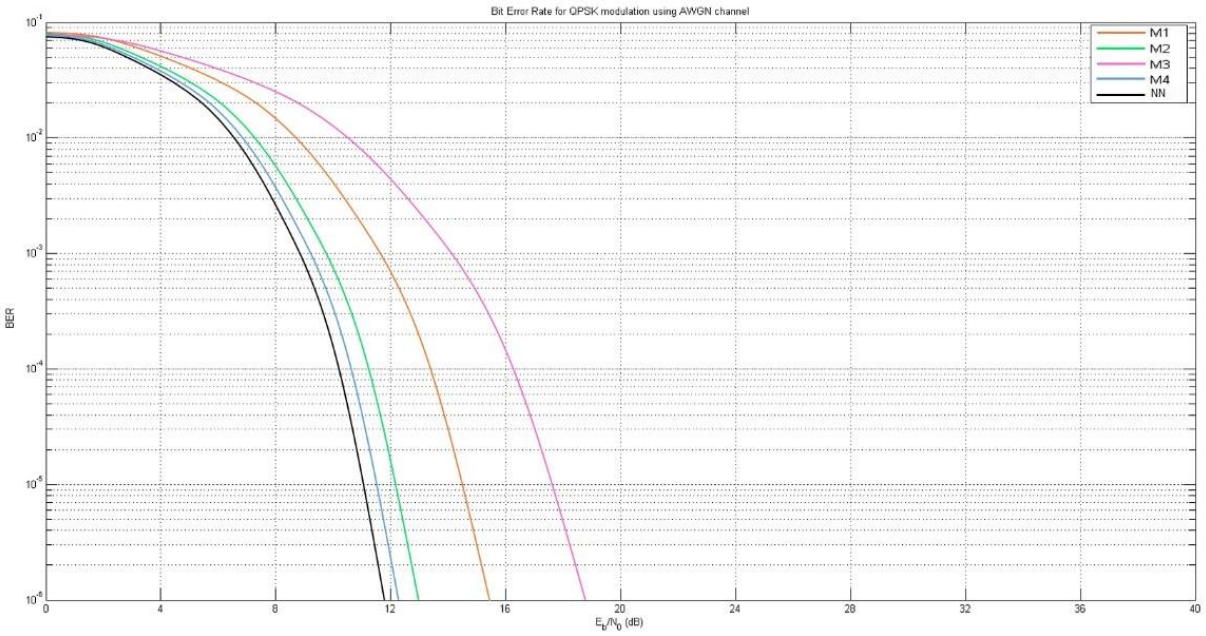

Fig. 34: A BER comparison between our optimised model and the four optimized models for Urban BS at 0.2km

6 OPTIMIZED MODEL DEPLOYMENT

A planned deployment in a Wireless Sensor Network (WSN) reveals the usefulness of developing an optimized propagation model for wireless telecommunications that serve cutting-edge applications during disaster relief, security, surveillance, traffic control, and Internet of Things (IoT) [41, 80-83]. Such an ad hoc network may contain several remote sensors that collect ground segment data as Fig. 35 illustrates. The link quality between a LAP sink and ground sensors depends on factors such as elevation angle between the LAP and the sensors, operation frequency, transmission power, transmit and receive antenna gains, RSS, atmospheric conditions, bit rate and link distance.

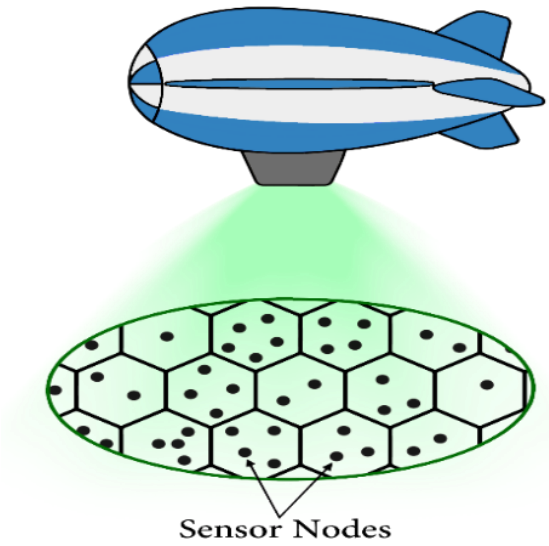

Fig. 35: LAP sink-WSNs architecture

The NN-optimized model resolves several WSN issues: channel impairments because of high path losses and fading, battery lifetime, propagation path loss. Therefore, an initial consideration of an optimized propagation model promises not only to extend the coverage range and reduce fading, but also to optimize power consumption without using sensor power enhancements or external power sources because of the low propagation path loss and high RSS. The performance of wireless ad hoc networks may be analysed by considering their two main QoS indicators: the energy per bit to noise power spectral density ratio (Eb/No) and the bit error rate (BER) which highlights the performance of different digital modulation schemes. These indicators are considered in the link budget to set QoS guarantees for the applications they serve. Setting the Equivalent Isotopically Radiated Power (EIRP) parameter values and path loss P_L from the initial four propagation models and the optimized model [41, 80, 81], the Eb/No can be expressed (in dBm) as:

$$\frac{E_b}{N_0} = \frac{C}{N} + 10\log BW - 10\log R_b \tag{39}$$

$$\frac{C}{N} = EIRP - P_L - A_R + \left(\frac{G}{T}\right) - 10\log\frac{K\,Bw}{0.001} \tag{40}$$

$$EIRP = P_t + G_t + G_r - L \tag{41}$$

$$\frac{G}{T} = G_r - 10\log T \tag{42}$$

where C/N is carrier power measured in dB, BW is bandwidth measured in Hz, R_b is the data rate of WiMAX for specific QPSK modulation and bandwidth value set at 6.048 Mb/s, EIRP is measured in dBm, transmitter power (P_t), transmitter antenna gains (G_t), receiver antenna gains (G_r) as well as (L) connector and cable loss, A_R is rain attenuation and atmospheric gas attenuation which are negligible, K is Boltzmann's constant (1.38065×10^{-23}), 0.001 represents a normalization, G/T the ratio of the receive antenna gain to system noise temperature measured in dB0, T is an effective temperature in this model (310K). The link performance indicator for signal quality is BER/Probability of Error which in turn is directly related to Eb/No. Thus, we calculate the BER as a function of Eb/No for a QPSK modulation in an AWGN channel as:

$$BER = \frac{1}{2}erfc\sqrt{\frac{E_b}{N_0}} \tag{43}$$

where *erfc* is a complementary error function that describes the cumulative probability curve of Gaussian distribution.

Simulations of the optimised and non-optimised propagation models have been mathematically modelled in MATLAB across different environments and LAP altitudes. Figures 36 to 41 show the predicted Eb/No results for both BS and HS for the four non-optimised and optimised propagation models at a 0.2km altitude across urban, suburban, and rural environments using the "semilogy" function in MATLAB. The simulation results on Table 5 show the Eb/No performance of all models at various LAP altitudes, receiver gains and across different environments at the lowest BER achieved of $1x10^{-6}$.

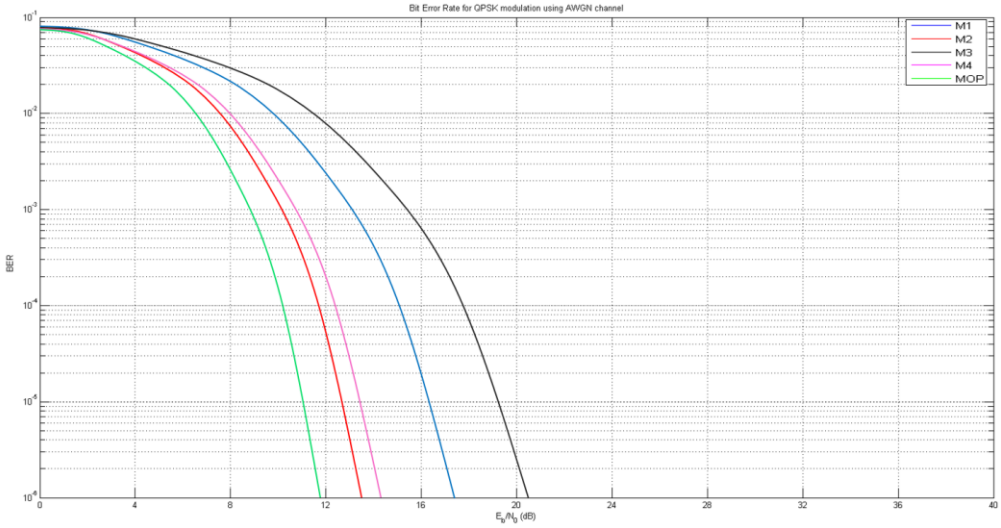

Fig. 36: BER of a signal as a function of Eb/No for Urban BS at 0.2km

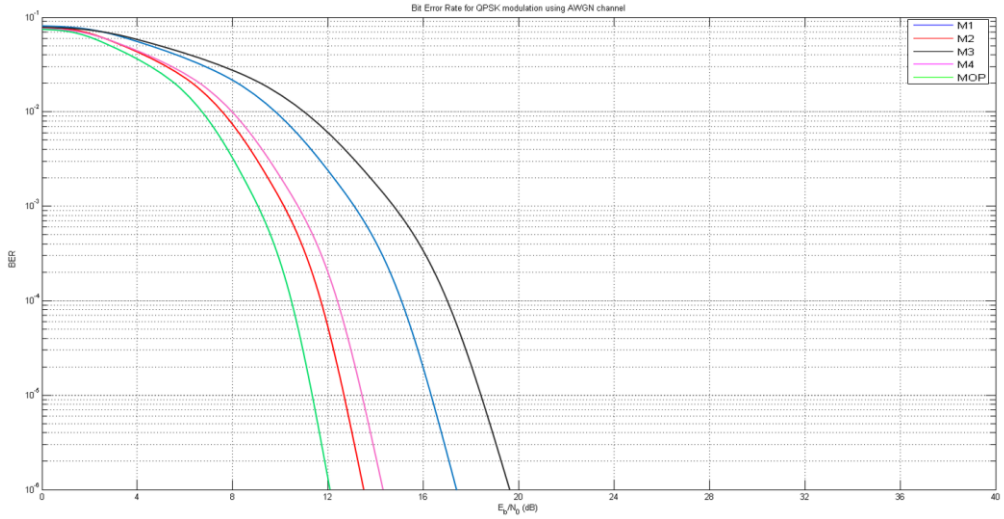

Fig. 37: BER of a signal as a function of Eb/No for Urban HS at 0.2km

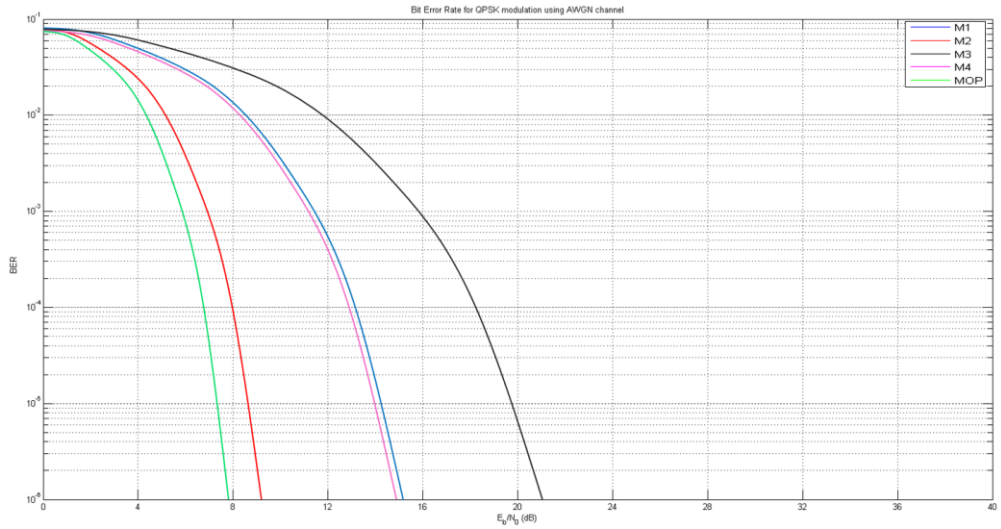

Fig. 38: BER of a signal as a function of Eb/No for Suburban BS at 0.2km

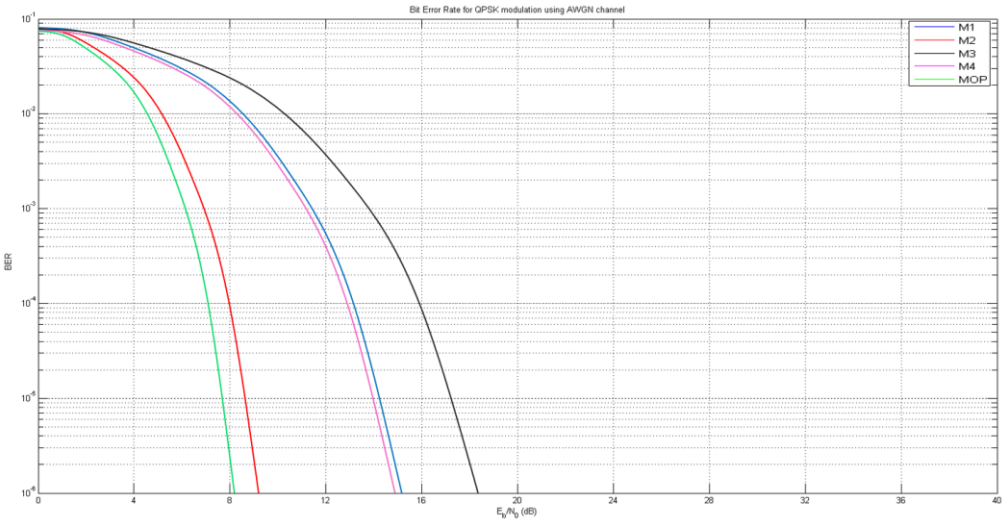

Fig. 39: BER of a signal as a function of Eb/No for Suburban HS at 0.2km

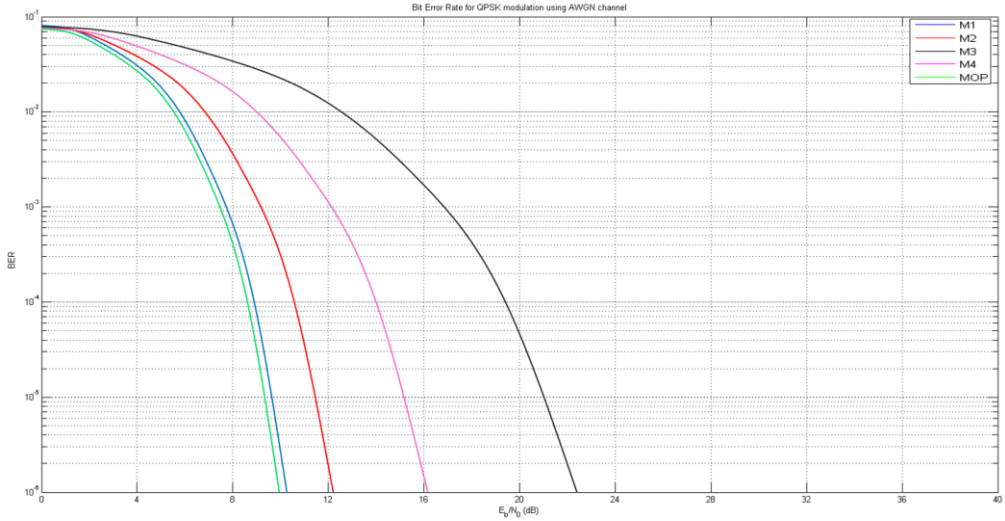

Fig. 40: BER of a signal as a function of Eb/No for Rural BS at 0.2km

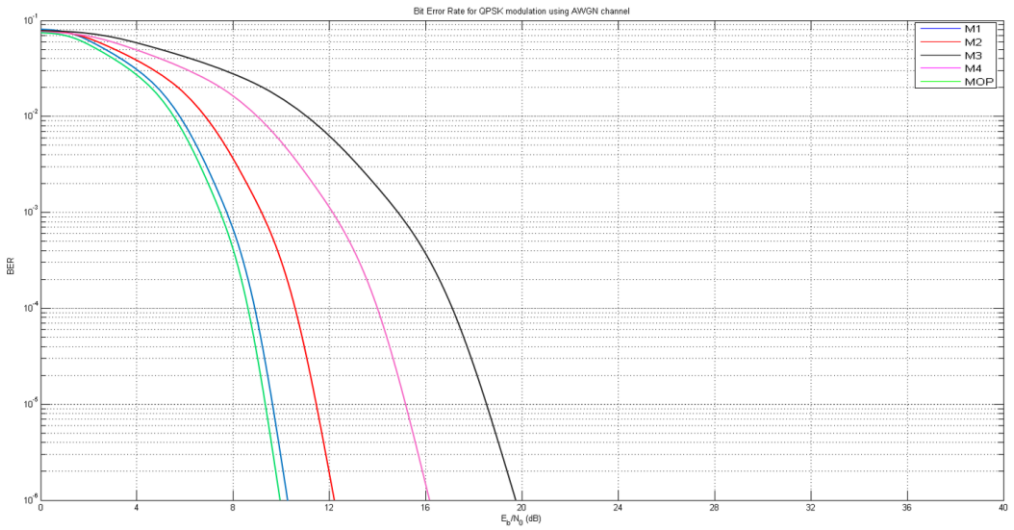

Fig. 41: BER of a signal as a function of Eb/No for Rural HS at 0.2km

Table 5: BER as a function of Eb/No @ 0.2km altitude

Model / *Parameter*	**M1**	**M2**	**M3**	**M4**	**MOP**
0.2km LAP Altitude - Large gain sensors (Urban)					
Eb/No **(dB)**	17.90	13.87	21.31	14.24	11.89
0.2km LAP Altitude - Small gain sensors (Urban)					
Eb/No (dB)	17.90	13.87	19.21	14.24	12.16
0.2km LAP Altitude - Large gain sensors (Suburban)					
Eb/No **(dB)**	15.23	9.07	21.02	15.04	7.86
0.2km LAP Altitude - Small gain sensors (Suburban)					
Eb/No **(dB)**	15.23	9.07	18.85	15.04	8.23
0.2km LAP Altitude - Large gain sensors (Rural)					
Eb/No **(dB)**	10.80	12.51	22.72	16.25	10.45
0.2km LAP Altitude - Small gain sensors (Rural)					
Eb/No **(dB)**	10.80	12.51	19.44	16.25	10.67
M1: ITU-R P.529-3 model, M2: Okumura model, M3: Hata-Davidson model, M4: ATG model, MOP: Optimised model					

The best link performance is the one that allows for the lowest possible BER with the lowest possible Eb/No. That prescribes a robust channel, where a low error rate is achieved without requiring a high transmission power. Figures 34 to 39 show that at the lowest BER $1x10^{-6}$, the optimised model, drawn in green, exhibits the lowest Eb/No with range floats between 0.5dB and 15dB which helps optimise performance. It is observed that as PL decreases, both BER and Eb/No decrease and system performance improves. Both the Okumura and ATG models exhibit the second best Eb/No performance after the optimised model due to their low PL across all environments and altitudes. Varying LAP altitudes with an increase in distance across different geomorphologies also affects BER and Eb/No. Unsurprisingly, small gain sensors perform better than larger ones because of antenna gains, but their transmission is suitable for shorter distances. The overall results of these two QoS indicators reveal reasonable improvements. This may lead to a reduction in the required transmission power from sensors and an improved link performance between LAP and ground sensors, thus, increasing network lifetime and performance.

7 CONCLUDING DISCUSSION AND FUTURE WORK

Propagation models are invaluable in the prediction of signal propagation loss between a transmitter and its receivers in locations where a wireless communication systems network has or is being deployed. Research work on near space platforms that considers empirical propagation models is sparse apart from that. This has motivated, on one hand, our selection of the empirical models considered in this paper and their suitability for last mile LAP connectivity, on the other hand. Consequently, each model has been customized to a close approximation of a LAP quasi-stationary condition at a specific realistic altitude. This included the elevation angle in calculating the coverage radius distance instead of the traditional approach of coverage calculation. The prediction results suggest that such a customization suits a LAP quasi-stationary condition. The simulation results predict significant improvements across the three environments at various altitudes. Finally, a WSN simulation study validates the optimized model performance in comparison to the other models as it yields the lowest Eb/No and lowest BER. This may lead to reduction in power consumption and improvements in link performance between LAP and ground sensors, thus, increasing the lifetime and performance of the network. Generating predictions in any location using a model that integrates Google Maps is gaining momentum.

7.1 Complexity Analysis

We use complexity theory to analyse, and Big-O notation to map, the complexity of our proposed ML framework's two main phases as can be seen on the optimisation flowchart on Fig. 42: Phase 1 that uses NN-SOMs, and Phase 2 that uses NNs Feedback Forward fitting tool to estimate the runtime behaviour in each phase. Our complexity approach focuses on the relationship between the number of basic operations with respect to the size of input, i.e. the number of iterations, and the number of LAP altitudes. The complexity functions are expressed as follows:

$$O_{Ph_1}(n) = n^2 + C_{Ph_1} \tag{44}$$

$$O_{Ph_1}(n) = n \times 2 + C_{Ph_2} \tag{45}$$

where $O_{ph}(n)$ denotes the complexity level, n is the number of operations, $C_{Ph_1} = 0.70$, and $C_{Ph_2} = 0.55$.

Fig. 43 demonstrates the level of complexity for the two phases and the overall complexity using the Big-O notation, which is an expression of how the execution time of a program scales with the input data. Clearly, the complexity figure shows that the number of iterations grows exponentially in relation to the number of LAP altitudes, as at each altitude height the number of parameters considered and used as inputs to NN especially during phase 1 increases in relation to the number of iterations until the input converges. Phase 1 yields a higher level of complexity in comparison to phase 2, partly due to the number of parameters at each LAP altitude in consideration during this phase, and partly due to the higher number of iterations. The overall complexity, therefore, increases in relation to the number of LAPs altitudes. Overall this suggests a medium level of complexity.

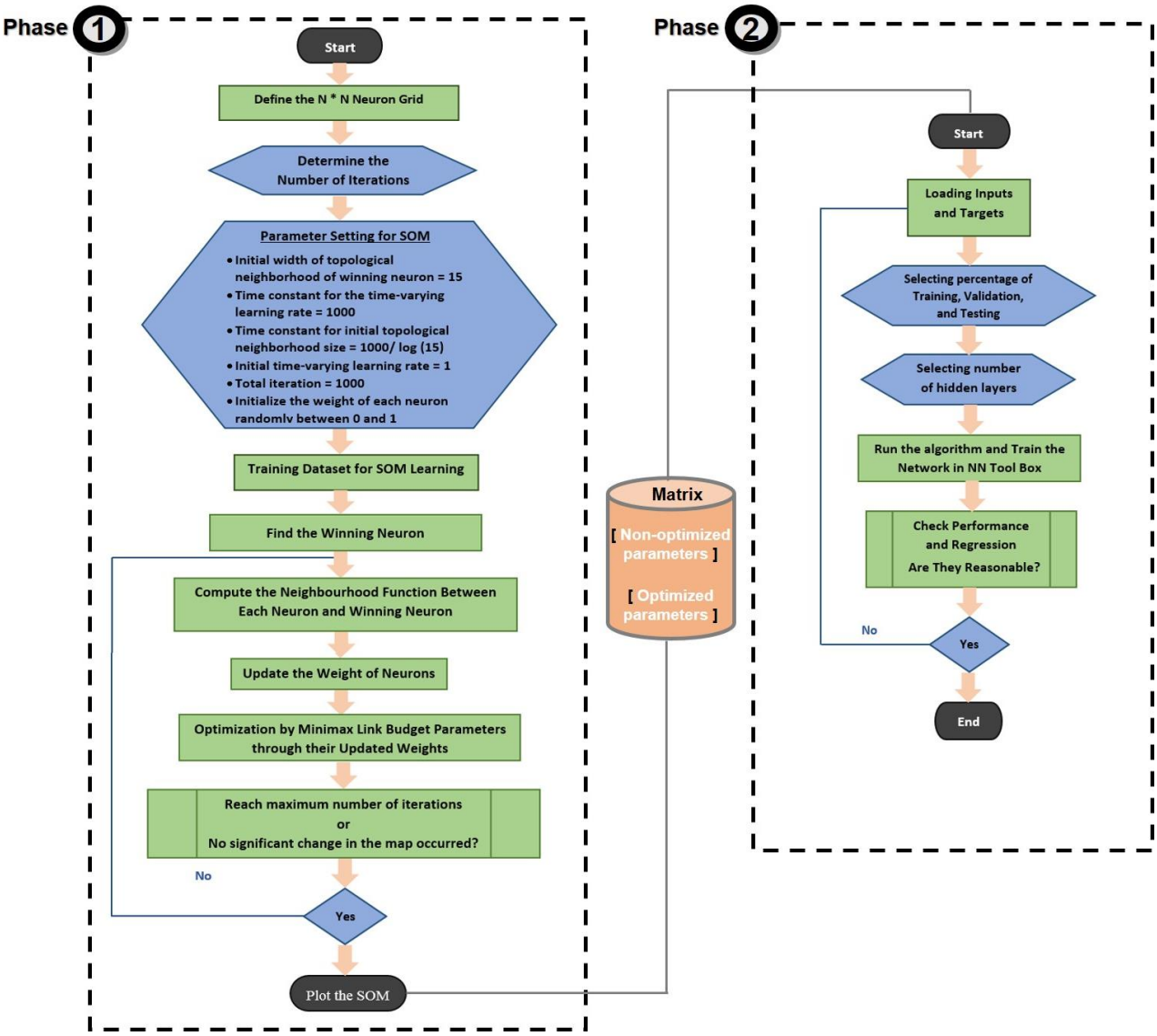

Fig. 42: Optimisation Flowchart

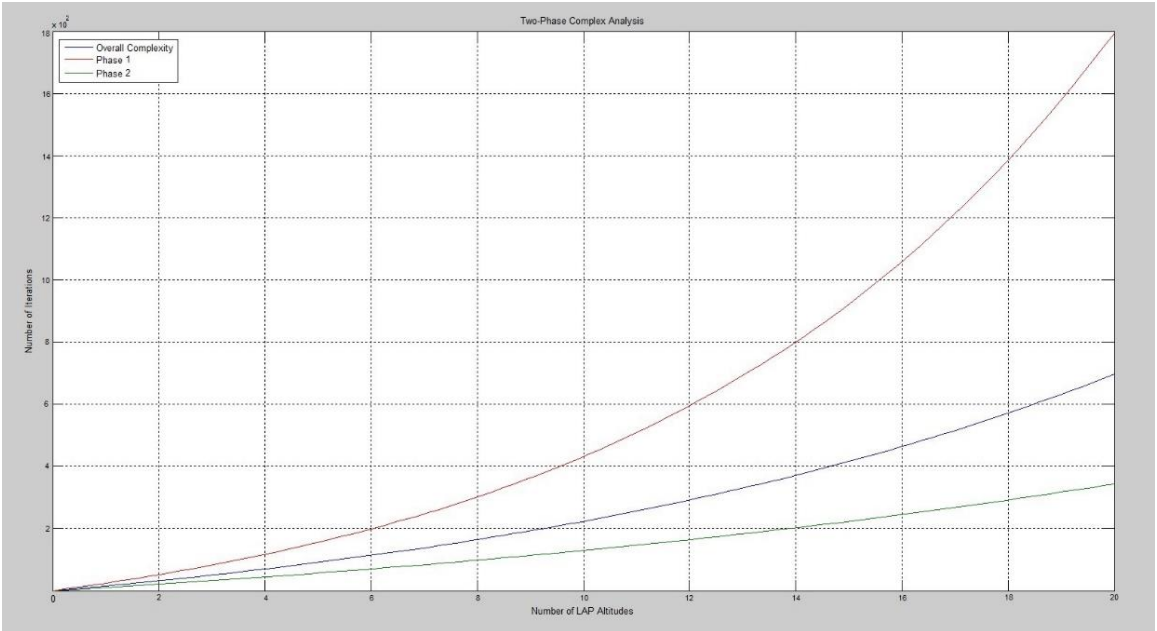

Fig. 43: Complexity Analysis

References

[1] D. Grace, T. Jiang, S. Allsopp, and L. Reynaud, “Integrated Project ABSOLUTE - Aerial Base Stations with Opportunistic Links for Unexpected & Temporary Events,” *IEEE Communications Magazine*, vol.54, no.4, pp.31-39, October 2013.

[2] A. Al-Hourani, S. Kandeepan, and S. Lardner, "Optimal LAP Altitude for Maximum Coverage," *IEEE Wireless Communications Letters*, vol.3, no.6, pp.569-572, Dec. 2014.

[3] S. H. Alsamhi, M. S. Ansari, O. Ma, F. Almalki and S. K. Gupta, “Tethered Balloon Technology in Design Solutions for Rescue and Relief Team Emergency Communication Services,” *Disaster Medicine and Public Health Preparedness*, pp.1-8, May 2018.

[4] A. Al-Hourani and S. Kandeepan, "Cognitive Relay Nodes for airborne LTE emergency networks," *7th International Conference on Signal Processing and Communication Systems (ICSPCS)*, Carrara, Australia, 2013, pp.1-9.

[5] J. Sánchez-García, J. García-Campos, M. Arzamendia, D. Reina, S. Toral and D. Gregor, "A survey on unmanned aerial and aquatic vehicle multi-hop networks: Wireless communications, evaluation tools and applications", *Computer Communications*, vol. 119, pp. 43-65, 2018.

[6] F. A. Almalki, M. C. Angelides, “Considering near space platforms to close the coverage gap in wireless communications; the case of the Kingdom of Saudi Arabia,” *FTC 2016 - Future Technologies Conference*, San Francisco, USA, 2016, pp.224 – 230.

[7] S. A. Khaleefa, S. H. Alsamhi, and N. S. Rajput, "Tethered balloon technology for telecommunication, coverage and path loss," *IEEE Students’ Conference on Electrical, Electronics and Computer Science*, Bhopal, India, 2014, pp.1-4.

[8] S. Alsamhi, S. Gapta, N. Rajput and R. Saket, "Network Architectures Exploiting Multiple Tethered Balloon Constellations for Coverage Extension," *6th International Conference on Advances in Engineering Sciences and Applied Mathematics (ICAESAM)*, Kuala Lumpur, Malaysia, 2016, pp.1-6.

[9] A. Rubina, O. Andryeyev, M. Harounabadi, A. Al-Khani, and O. Artemenko, "Investigation and Adaptation of Signal Propagation Models for a Mixed Outdoor-Indoor Scenario Using a Flying GSM Base Station," *Springer Ad Hoc Networks*, Ottawa, vol.184, pp.128-139, Dec. 2016.

[10] S. Chandrasekharan, A. Al-Hourani, K. Gomez, S. Kandeepan, R. Evans, L. Reynaud, and S. Scalise, "Performance Evaluation of LTE and WiFi Technologies in Aerial Networks," *IEEE Globecom Workshops (GC Wkshps),Washington*, USA, 2016, pp.1-7.

[11] A. Al-Hourani, S. Kandeepan, and A. Jamalipour, "Modeling air-to-ground path loss for low altitude platforms in urban environments," *2014 IEEE Global Communications Conference*, Austin, USA, 2014, pp.2898-2904.

[12] K. Gomez, A. Hourani, L. Goratti, R. Riggio, S. Kandeepan, I. Bucaille, "Capacity evaluation of Aerial LTE base-stations for public safety communications," *European Conference on Networks and Communications (EuCNC)*, Paris, France, 2015, pp.133-138.

[13] L. Zhao, J. Yi, F. Adachi, C. Zhang, and H. Zhang, "Power-Efficient Radio Resource Allocation for Low-Medium-Altitude Aerial Platform Based TD-LTE Networks," *IEEE Vehicular Technology Conference (VTC Fall)*, Quebec, Canada, 2012, pp.1-4.

[14] D. Nalineswari and N. Rakesh, "Link budget analysis on various terrains using IEEE 802.16 WIMAX standard for 3.5 GHz frequency," *IEEE International Conference on Electrical, Computer and Communication Technologies (ICECCT)*, Coimbatore, India, 2015, pp.1-5.

[15] C. Phillips, D. Sicker, and D. Grunwald, "A survey of wireless path loss prediction and coverage mapping methods," *IEEE Communications Surveys & Tutorials*, vol.15, no.1, pp.255-270, 2013.

[16] W. Khawaja, I. Guvenc, D. Matolak, U. C. Fiebig, and N. Schneckenberger, “A survey of air-to-ground propagation channel modeling for unmanned aerial vehicles,” *arXiv, Electrical Engineering and Systems*, vol. *1801*, no. *016*, pp.1-25, 2018.

[17] H. Shakhatreh, A. Sawalmeh, A. Al-Fuqaha, Z. Dou, E. Almaita, I. Khalil, N. Othman, A. Khreishah, M. Guizani, "Unmanned Aerial Vehicles: A Survey on Civil Applications and Key Research Challenges," *arXiv, Electrical Engineering and Systems*, vol. *1805*, no.00881, pp.1-58, 2018.

[18]A. Khuwaja, Y. Chen, N. Zhao, M. Alouini and P. Dobbins, "A Survey of Channel Modeling for UAV Communications", *IEEE Communications Surveys & Tutorials*, vol. 20, no. 4, pp. 2804-2821, 2018.

[19] J. Wu, "A multi-tiered network with aerial and ground coverage", *Computer Communications*, vol. 131, pp. 39-42, 2018.

[20] M. Younis, "Internet of everything and everybody: Architecture and service virtualization", *Computer Communications*, vol. 131, pp. 66-72, 2018.

[21] B. Li, Z. Fei and Y. Zhang, "UAV Communications for 5G and Beyond: Recent Advances and Future Trends", *IEEE Internet of Things Journal*, pp. 1-53, 2019.

[22] J. S. Seybold, *Introduction to RF propagation*. United Kingdom: Wiley-Blackwell Ney jersy, USA, 2005.

[23] D. Grace and M. Mohorcic, *Broadband communications via high-altitude platforms*. United Kingdom: Wiley-Blackwell (an imprint of John Wiley & Sons Ltd), 2010.

[24] A. Aragón-Zavala, J. Cuevas-Ruíz, and J. Delgado-Penín, *High-altitude platform systems for wireless communications*. United Kingdom: Wiley-Blackwell (an imprint of John Wiley & Sons Ltd), 2008.

[25] N. Sharma, M. Magarini, L. Dossi, L. Reggiani and R. Nebuloni, "A study of channel model parameters for aerial base stations at 2.4 GHz in different environments", *15th IEEE Annual Consumer Communications & Networking Conference (CCNC)*, Las Vegas, USA 2018, pp.1 - 6.

[26] J. Holis and P. Pechac, "Elevation dependent shadowing model for mobile communications via high altitude platforms in built-up areas," *IEEE Transactions on Antennas and Propagation*, vol.56, pp.1078-1084, April 2008.

[27] A. Al-Hourani and K. Gomez, "Modeling Cellular-to-UAV Path-Loss for Suburban Environments", *IEEE Wireless Communications Letters*, vol. 7, no. 1, pp. 82-85, 2018.

[28] D. G. Cileo, N. Sharma, and M. Magarini, "Coverage, capacity and interference analysis for an aerial base station in different environments," *IEEE International Symposium on Wireless Communication Systems (ISWCS)*, Bologna, Italy Aug 2017, pp. 281–286.

[29] A. Habib, "MIMO Channel Modeling for Integrated High Altitude Platforms , Geostationary Satellite / Land Mobile Satellite and Wireless Terrestrial Networks," *Journal of Space Technology*, vol.3, pp.19-26, July 2013.

[30] A. Mohammed, A. Mehmood, F.-N. Pavlidou, and M. Mohorcic, "The Role of High-Altitude Platforms (HAPs) in the Global Wireless Connectivity," *Proceedings of the IEEE*, vol.99, no.11, pp.1939-1953, Aug. 2011.

[31] S. Chandrasekharan, K. Gomez, A. Al-Hourani, S. Kandeepan, T. Rasheed, L. Goratti, L. Reynaud, D. Grace, I. Bucaille, T. Wirth, and S. Allsopp, "Designing and implementing future aerial communication networks," *IEEE Communications Magazine*, vol.54, no.5, pp.26-34, May 2016.

[32] I. Dalmasso,I. Galletti, R. Giuliano, F. Mazzenga, "WiMAX networks for emergency management based on UAVs," *2012 IEEE First AESS European Conference on Satellite Telecommunications*, Rome, Italy, 2012, pp.1-6.

[33] A. Kumbhar, I. Guvenc, S. Singh and A. Tuncer, "Exploiting LTE-Advanced HetNets and FeICIC for UAV-Assisted Public Safety Communications", *IEEE Access*, vol. 6, no.1 , pp. 783-796, 2018.

[34] M. Mozaffari, W. Saad, M. Bennis, Y.-H. Nam, and M. Debbah, "A tutorial on UAVs for wireless networks: Applications, challenges, and open problems," arXiv, *Electrical Engineering and Systems*, vol. 1803, no. 00680, pp.1-23, 2018.

[35] J. Oueis, V. Conan, D. Lavaux, H. Rivano, R. Stanica and F. Valois, "Core network function placement in self-deployable mobile networks", *Computer Communications*, vol. 133, pp. 12-23, 2019.

[36] S. Alsamhi, O. Ma, M. Ansari and S. Gupta, "Collaboration of Drone and Internet of Public Safety Things in Smart Cities: An Overview of QoS and Network Performance Optimization", *Drones*, vol. 3, no. 1, p. 13, 2019.

[37] T. Li, K. Ota, T. Wang, X. Li, Z. Cai and A. Liu, "Optimizing the Coverage via the UAVs with Lower Costs for Information-Centric Internet of Things", *IEEE Access*, pp. 1-17, 2019.

[38] N. Hossein Motlagh, T. Taleb and O. Arouk, "*Low-Altitude Unmanned Aerial Vehicles-Based Internet of Things Services: Comprehensive Survey and Future Perspectives*", IEEE Internet of Things Journal, vol.3, no.6, pp.899-922, Dec. 2016.

[39] K. M. Gajra and R. S. Pant, "SoPTAS: Solar powered tethered aerostat system," *1st International Conference on Non-Conventional Energy (ICONCE 2014)*, Kalyani, India, 2014, pp.65-68.

[40] I. Bucaille,S. Hethuin, T. Rasheed, A. Munari, R. Hermenier, and S. Allsopp, "Rapidly Deployable Network for Tactical Applications: Aerial Base Station with Opportunistic Links for Unattended and Temporary Events ABSOLUTE Example," *MILCOM 2013 - IEEE Military Communications Conference*, San Diego, USA, 2013, pp.1116-1120.

[41] S. Zhang, Z. Wang, M. Qiu and M. Liu, "*BER-based Power Scheduling in Wireless Sensor Networks*," Journal of Signal Processing Systems, vol.72, no.3, pp.197-208, September 2013.

[42] D. Duan, "Optimizing the Battery Energy Efficiency in Wireless Sensor Networks," *IEEE International Conference on Signal Processing, Communications and Computing (ICSPCC)*, Xi'an, China, 2011, pp.1-6.

[43] O. Andryeyev, O. Artemenko and A. Mitschele-Thiel, "Improving the System Capacity Using Directional Antennas with a Fixed Beam on Small Unmanned Aerial Vehicles," *European Conference on Networks and Communications (EuCNC)*, Paris, France, 2015, pp.139-143.

[44] F. Teixeira, "Tethered Balloons and TV White Spaces: A Solution for Real-time Marine Data Transfer at Remote Ocean Areas," *IEEE Third Underwater Communications and Networking Conference (UComms)*, Lerici, Italy, 2016, pp.1-5.

[45] A. Al-Kandari, M. Al-Nasheet, and A. R. Abdulgafer, "WiMAX vs. LTE: An analytic comparison," *Fourth International Conference on Digital Information and Communication Technology and its Applications (DICTAP)*, Bangkok, Thailand, 2014, pp.389-393.

[46] U. R. Mori,P. Chandarana, G. Gajjar, and S.Dasi , "Performance comparison of different modulation schemes in advanced technologies WiMAX and LTE," *IEEE International Advance Computing Conference (IACC)*, Banglore, India, 2015, pp.286-289.

[47] I. Aldmour, "LTE and WiMAX: Comparison and future perspective," *Communications and Network*, vol.5, no.4, pp.360-368, Oct. 2013.

[48] L. Reynaud and T. Rasheed, "Deployable aerial communication networks," *ACM symposium on Performance evaluation of wireless ad hoc, sensor, and ubiquitous networks - PE-WASUN '12*, Paphos, Cyprus, 2012, pp.9-16.

[49] A. Guillen-Perez, R. Sanchez-Iborra, M. Cano, J. Sanchez-Aarnoutse, and J.Garcia-Haro, "WiFi NETWORKS ON DRONES," *ITU Kaleidoscope: ICTs for a Sustainable World (ITU WT)*, Bangkok Thailand, 2017, pp.1-8.

[50] K. Gomez, T. Rasheed, L. Reynaud, and S. Kandeepan, "On the performance of aerial LTE base-stations for public safety and emergency recovery," *IEEE Globecom Workshops (GC Wkshps)*, Atlanta,USA, 2013, pp.1391-1396.

[51] M. A. Rahman, "Enabling drone communications with WiMAX Technology," *IISA 2014, The 5th International Conference on Information, Intelligence, Systems and Applications*, Chania, Greece, 2014, pp.323-328.

[52] F. A. Almalki, M. C. Angelides, "Empirical Evolution of a Propagation Model for Low Altitude Platforms", *Computing Conference 2017*, London, UK, July 2017, pp.1297-1304.

[53] Iskandar and A. Abubaker, "Co-channel interference mitigation technique for mobile WiMAX downlink system deployed via Stratospheric Platform," *8th International Conference on Telecommunication Systems Services and Applications (TSSA)*, Kuta, Indonesia, 2014, pp.1-5.

[54] Z. Yang and A. Mohammed, "Deployment and capacity of mobile WiMAX from high altitude platform," *2011 IEEE Vehicular Technology Conference (VTC Fall)*, San Francisco, USA, 2011, pp.1-5.

[55] D. Yuniarti, "Regulatory challenges of broadband communication services from High Altitude Platforms (HAPs)", *International Conference on Information and Communications Technology (ICOIACT)*, Yogyakarta, Indonesia, 2018, pp.919 -922.

[56] N. Zhao, X. Yang, A. Ren, Z. Zhang, W. Zhao, F. Hu, M. Ur Rehman, H. Abbas and M. Abolhasan, "Antenna and Propagation Considerations for Amateur UAV Monitoring", *IEEE Access*, vol. 6, no.1, pp. 28001-28007, 2018.

[57] C., Robert M, *The technical collection of intelligence*. Washington, DC: CQ Press, 2010.

[58] S. Ghafoor, P. Sutton, C. Sreenan, and K. Brown, "Cognitive radio for disaster response networks: survey, potential, and challenges," *IEEE Wireless Communications*, vol.21, no.5, pp.70-80, Jan. 2014.

[59] H. Sharma and B. P, "A communication approach for aerial surveillance of long linear infrastructures in non-urban terrain," *Twenty First National Conference on Communications (NCC)*, Mumbai, India, 2015, pp.1-6.

[60] H. Li, X. Xu, M. Yang, and Q. Guo, "Compensative mechanism based on steerable antennas for High Altitude Platform movement," *6th International ICST Conference on Communications and Networking in China (CHINACOM)*, Harbin, China, 2011, pp.870-874.

[61] M. Silva, A. Correia, R. Dinis, N. Souto, J. Silva, *Transmission techniques for emergent multicast and broadcast systems.* Boca Raton, FL: CRC Press / Taylor & Francis, 2010.

[62] L. L. Hanzo, *MIMO-OFDM for LTE, Wi-Fi, and WiMAX: Coherent versus non-coherent and cooperative turbo-transceivers*. United States: John Wiley & Sons, 2011.

[63] Y. Shi, R. Enami, J. Wensowitch, and J. Camp, "UABeam: UAV-Based beamforming system analysis with in-field airto-ground channels," in Proc. of IEEE International Conference on Sensing, Communication, and Networking (SECON), Hong Kong, China, June 2018, pp. 1–9.

[64] W. Feng, J. Wang, Y. Chen, X. Wang, N. Ge and J. Lu, "UAV-Aided MIMO Communications for 5G Internet of Things", *IEEE Internet of Things Journal*, vol.1, no.1, pp. 1-10, 2018.

[65] N. Rakesh, B. Maheswari, and S. Srivatsa, "Performance analysis of propagation models in different terrain conditions for IEEE standard 802.16e WiMAX," *International Conference on Communication and Signal Processing*, Melmaruvathur, India, 2014, pp.142-146.

[66] N. Rakesh and D. Nalineswari, "Comprehensive performance analysis of path loss models on GSM 940 MHz and IEEE 802.16 WIMAX frequency 3.5 GHz on different terrains," *International Conference on Computer Communication and Informatics*, Coimbatore, India, 2015, pp.1-7.

[67] M. Lustgarten and J. Madison, "An empirical propagation model (EPM-73)," *IEEE Transactions on Electromagnetic Compatibility*, vol.19, no.3, pp.301-309, Aug. 1977.

[68] Q. Feng, J. Mcgeehan, E. Tameh, and A. Nix, "Path loss models for air-to-ground radio channels in urban environments," *IEEE 63rd Vehicular Technology Conference*, Melbourne, Australia, 2006, pp.2901-2905.

[69] ITU Radiocommunication Bureau (BR), "F.1500 - preferred characteristics of systems in the fixed service (FS) using high altitude platforms operating in the bands 47.2-47.5 GHz and 47.9-48.2 GHz," 2010. [Online]. Available: https://www.itu.int/dms_pubrec/itu-r/rec/f/R-REC-F.1500-0-200005-I!!PDF-E.pdf. Accessed: May 11, 2016.

[70] M. Mozaffari, W. Saad, M. Bennis, and M. Debbah, "Drone small cells in the clouds: Design, deployment and performance analysis," *IEEE Global Communications Conference*, San Diego, USA, 2015, pp.1-6.

[71] W. L. Tan, P. Hu, and M. Portmann, "Experimental evaluation of measurement-based SINR interference models," *IEEE International Symposium on a World of Wireless, Mobile and Multimedia Networks (WoWMoM)*, San Francisco, USA, 2012, pp.1-9.

[72] M. Malkowski, "Link-level comparison of IP-OFDMA (mobile WiMAX) and UMTS HSDPA," *IEEE 18th International Symposium on Personal, Indoor and Mobile Radio Communications*, Athens, Greece, 2007, pp.1-5.

[73] "Airspan networks, leaders in 4G technology,". [Online]. Available: http://www.airspan.com/about-airspan/. Accessed [Jan. 10, 2016].

[74] K. Raivio, O. Simula, J. Laiho, and P. Lehtimaki, "Analysis of mobile radio access network using the self-organizing map," *IFIP/IEEE Eighth International Symposium on Integrated Network Management,*Colorado Springs, USA, 2003, pp.439 - 451.

[75] "Computation visualization programming neural network Toolbox for use with MATLAB.

[76] Y. Lin and H. Ye, "Input Data Representation for Self-Organizing Map in Software Classification," *Second International Symposium on Knowledge Acquisition and Modeling*, Wuhan, China, 2009, pp.350 - 353.

[77] Y. Lin and H. Ye, "Input Data Representation for Self-Organizing Map in Software Classification", IEEE *Second International Symposium on Knowledge Acquisition and Modeling*, Wuhan, China, Dec. 2009, pp.163–195.

[78] V. Jain, A. Singh, V. Chauhan, and A. Pandey, "Analytical study of wind power prediction system by using feed forward neural network," *International Conference on Computation of Power, Energy Information and Communication (ICCPEIC)*, Chennai, India, 2016, pp.303-306.

[79] R. Singh and S. Kansal, "Artificial neural network-based spectrum recognition in cognitive radio," *IEEE Students' Conference on Electrical, Electronics and Computer Science*, Bhopal, India, 2016, pp.1-6.

[80] Z. Yang and A. Mohammed, "High Altitude Platforms for Wireless Sensor Network applications," IEEE International Symposium on Wireless Communication Systems, Reykjavik, Iceland, 2008, pp.613 - 617.

[81] F. Almalki, M. Angelides, "Propagation modelling and performance assessment of aerial platforms deployed during emergencies," *12th IEEE International Conference for Internet Technology and Secured Transactions (ICITST-2017)*, Cambridge, UK, 2017, pp.238–243.

[82] Y. Albagory and O. Said, "Performance enhancement of high-altitude platforms wireless sensor networks using concentric circular arrays," *AEU - International Journal of Electronics and Communications*, vol.69, no.1, pp.382-388, January 2015.

[83] M. Poulakis, S. Vassaki and A. Panagopoulos, "Satellite-Based Wireless Sensor Networks: Radio Communication Link Design", *7th European Conference on Antennas and Propagation (EuCAP)*, Sweden, 2013.